МІНІСТЕРСТВО ОСВІТИ І НАУКИ УКРАЇНИ
НАЦІОНАЛЬНИЙ АВІАЦІЙНИЙ УНІВЕРСИТЕТ
ФАКУЛЬТЕТ АЕРОНАВІГАЦІЇ, ЕЛЕКТРОНІКИ ТА ТЕЛЕКОМУНІКАЦІЙ
КАФЕДРА АЕРОКОСМІЧНИХ СИСТЕМ УПРАВЛІННЯ

ДОПУСТИТИ ДО ЗАХИСТУ
Завідувач кафедри
______________Юрій МЕЛЬНИК
«_____» ___________2024 р.

КВАЛІФІКАЦІЙНА РОБОТА

(ПОЯСНЮВАЛЬНА ЗАПИСКА)

ВИПУСКНИКА ОСВІТНЬОГО СТУПЕНЯ
«БАКАЛАВР»

Тема: «**Моделювання інтегруючого режиму роботи мікро-електро-механічного гіроскопа**»

Виконавець: студент групи СУ-404 ___________ Максим ТЕРЕЛЯК

Керівник: професор _______________________ Валерій ЧІКОВАНІ

Нормоконтролер: ____________________ Микола ДИВНИЧ

Київ 2024

MINISTRY OF EDUCATION AND SCIENCE OF UKRAINE
NATIONAL AVIATION UNIVERSITY
FACULTY OF AIR NAVIGATION, ELECTRONICS AND TELECOMMUNICATIONS
AEROSPACE CONTROL SYSTEMS DEPARTMENT

APPROVED FOR DEFENCE
Head of the Department
________________ Yurii MELNYK
“____” _____________ 2024

QUALIFICATION PAPER

(EXPLANATORY NOTE)

FOR THE ACADEMIC DEGREE OF BACHELOR

Title: **“Simulation of the rate-integrating mode of operation of a micro-electro-mechanical gyroscope”**

Submitted by: student of group CS-404 _____________ Maksym TERELYAK

Supervisor: professor _____________________ Valerii CHIKOVANI

Standards inspector: __________________________ Mykola DYVNYCH

Kyiv 2024

НАЦІОНАЛЬНИЙ АВІАЦІЙНИЙ УНІВЕРСИТЕТ

Факультет аеронавігації, електроніки та телекомунікацій

Кафедра аерокосмічних систем управління

Спеціальність: 151 «Автоматизація та комп'ютерно-інтегровані технології»

ЗАТВЕРДЖУЮ

Завідувач кафедри

_____________ Юрій МЕЛЬНИК

«_____»___________2024 р.

ЗАВДАННЯ

на виконання кваліфікаційної роботи

Тереляка Максима Стефановича

1. Тема кваліфікаційної роботи «Моделювання інтегруючого режиму роботи мікро-електро-механічного гіроскопа» затверджена наказом ректора від «01» квітня 2024 р. № 511/ст.

2. Термін виконання роботи: з 13.05.2024 по 16.06.2024.

3. Вихідні дані роботи: Блок-схема інтегруючого режиму роботи вібраційного гіроскопа та її Симулінк модель.

4. Зміст пояснювальної записки: Вступ, розділ 1- мікро-електро-механічні (МЕМС) гіроскопи, розділ 2 – режими роботи МЕМС гіроскопів, розділ 3 – результати моделювання інтегруючого режиму роботи, висновки, література.

5. Перелік обов’язкового ілюстративного матеріалу: Блок схеми, Симулінк модель, презентація у Power point.

6. Календарний план-графік

№ пор.	Завдання	Термін виконання	Відмітка про виконання
1	Отримання теми дипломної роботи	13.05.2024	Виконано
2	Написання першого розділу роботи	17.05.2024	Виконано
3	Написання другого розділу роботи	27.05.2024	Виконано
4	Подача керівнику першого та другого розділів на перевірку	28.05.2024	Виконано
5	Написання третього розділу роботи	7.06.2024	Виконано
6	Подача керівнику третього розділу на перевірку	8.06.2024	Виконано
7	Оформлення дипломної роботи	12.06.2024	Виконано
8	Підготовка презентації доповіді	16.06.2024	Виконано

7. Дата видачі завдання: «13» травня 2024 р.

Керівник кваліфікаційної роботи ____________________ Валерій ЧІКОВАНІ
(підпис керівника)

Завдання прийняв до виконання ______________________ Максим ТЕРЕЛЯК
(підпис випускника)

NATIONAL AVIATION UNIVERSITY

Faculty of Air Navigation, Electronics and Telecommunications

Aerospace Control Systems Department

Specialty: 151 “Automation and Computer-integrated Technologies”

APPROVED BY

Head of the Department

_____________ Yurii MELNYK

“_____”______________2024

Qualification Paper Assignment for Graduate Student

Terelyak Maksym Stefanovych

1. The qualification paper title “Simulation of the rate-integrating mode of operation of a micro-electro-mechanical gyroscope” was approved by the Rector’s order of “ 01 ” April 2024 № 511/ст.

2. The paper to be completed between: 13.05.2024 and 16.06.2024

3. Initial data for the paper: The rate-integration mode of operation block diagram and its Simulink model

4. The content of the explanatory note: Introduction, chapter 1 - micro-electro-mechanical (MEMS) gyroscopes, chapter 2 - operating modes of MEMS gyroscopes, chapter 3 - simulation results of the integrating mode of operation, conclusion, references

5. The list of mandatory illustrations: Block diagrams, Simulink model, presentation in Power point.

6. Timetable

№	Assignment	Dates of completion	Completion mark
1	Obtaining a thesis topic	13.05.2024	Done
2	Writing the first chapter of the work	17.05.2024	Done
3	Writing the second chapter of the work	27.05.2024	Done
4	Submitting the first and second sections to the manager for review	28.05.2024	Done
5	Writing the third chapter of the work	7.06.2024	Done
6	Submission to the head of the third section for review	8.06.2024	Done
7	Completion of the thesis	12.06.2024	Done
8	Preparation of the presentation of the report	16.06.2024	Done

7. Assignment issue date: “13” May 2024

Qualification paper supervisor ______________________ Valerii CHIKOVANI
(the supervisor’s signature)

Issued task accepted ______________________ Maksym TERELYAK
(the graduate student’s signature)

РЕФЕРАТ

Пояснювальна записка до дипломної роботи "Моделювання інтегруючого режиму роботи мікро-електро-механічного гіроскопа" містить 70 сторінок, 24 ілюстрацій, 29 джерел.

Актуальність теми полягає у необхідності вдосконалення точності та надійності інтегруючих гіроскопів для застосування їх у вимірювальних системах, автономних навігаційних системах рухомих об’єктів та інших високоточних пристроях, де вимагається стійка робота на довгі періоди часу.

Об'єктом дослідження є інтегруючий режим роботи мікро-електро-механічного гіроскопа.

Предметом дослідження є особливості симуляції та аналізу періодичних похибок в інтегруючому режимі вібраційного гіроскопа.

Метою роботи є визначення характеристик періодичних похибок в режимі інтегруючого гіроскопа за допомогою комп’ютерного моделювання та методів аналізу даних моделювання.

Методи дослідження моделювання в Simulink, метод найменших квадратів для вилучення похибок, аналіз даних, методи апроксимації складних функцій.

Ключові слова: ІНТЕГРУЮЧИЙ РЕЖИМ, МІКРО-ЕЛЕКТРО-МЕХАНІЧНИЙ ГІРОСКОП, МОДЕЛЮВАННЯ, ПЕРІОДИЧНІ ПОХИБКИ, МЕТОД НАЙМЕНШИХ КВАДРАТІВ, АНАЛІЗ ДАНИХ.

ABSTRACT

Explanatory note for the qualification paper "Simulation of the rate-integrating mode of operation of a micro-electro-mechanical gyroscope" includes: 70 pages, 24 illustrations, 29 sources.

The relevance of the topic is in the need to improve the accuracy and reliability of integrating gyroscopes for their use in measuring systems, autonomous navigation systems of vehicles, and other high-precision devices that require stable operation for long periods of time.

The object of the study is the integrating mode of operation of the micro-electro-mechanical gyroscope.

The subject of the research is features of simulation and analysis of periodic errors in the integrating mode of the vibrating gyroscope.

The aim of the work is the determination of the characteristics of periodic errors in the rate-integrating gyroscope using computer simulation and methods of simulation data analysis

Research methods include Simulink modeling, least squares method for error extraction, data analysis, and complex function approximation methods.

Key words: INTEGRATING MODE, MICRO-ELECTRO-MECHANICAL GYROSCOPE, MODELING, PERIODIC ERRORS, LEAST SQUARES METHOD, DATA ANALYSIS.

CONTENT

INTRODUCTION

Gyroscopes based on microelectromechanical systems, MEMS gyroscopes, are miniaturized variants of Coriolis vibratory gyros (CVG). Miniaturization is when a vibrating structure is made of a thin film of different materials. Because MEMS technology was borne inside the semiconductor integrated circuit industry, they are, first of all, silicon, polysilicon, amorphous silicon, and quarts materials which are usually deposited as thin films. Apart from these, silicon-compatible materials like silicon dioxides, silicon nitrides, carbides, glasses, and metals such as aluminum, titanium, tungsten, and copper are also used. Moreover, polymers such as photoresist and polyimide and other new materials appearing in new designs suitable for different applications are actively used in this industry, as well.

MEMS gyroscope’s sensing elements (SE) look like microcircuits and are amenable to mass production, borrowing technological processes from the semiconductor industry. Mass production of such gyros gives low-cost and miniature size expands applications and initiates big sales, even if the performances are moderate.

There are many practical implementations of the MEMS gyros, which can be used to produce a gyroscope as a rate sensor. However, it is expedient to overview in this section three types of them – tuning fork as one of the popular designs, flat highly symmetric vibrating ring designs, and as a modern technological achievement vibrating shell designs. By correct design of a highly symmetric shell or ring resonator, it is possible to overcome problems of its resonator sensitivity to imperfect mounting it to the casing experienced by more simple oscillators and thus improve bias performance, and greatly reduce sensitivity to shock and vibration.

As a device for measuring the angular rate of moving objects, the gyroscope is widely used in civil and military areas, such as aerospace, automobile, consumer electronics, ship navigation, and guided ammunition. Motivated by high performance large-scale gyroscopes, with the emergences and developments of micro-electro-mechanical system (MEMS) and micro-opto-electro-mechanical (MOEMS) system technologies, a new generation of the micro-gyroscope based on such MEMS technologies has become one of the focused development directions in the academic and industrial areas. MEMS/MOEMS gyroscopes have developed rapidly since the Draper Laboratory produced the first non-rotor silicon micromechanical gyroscopes in 1988. In the past several years, with the continuous developments of MEMS processing technologies, the performances of silicon MEMS gyroscopes based on different principles, structures, and materials have been greatly improved, mainly including the mechanical micro-gyroscopes based on Coriolis principles or angular momentum conservation.

Before the progress analysis on micro-gyroscopes, the main performance indexes, including the bias instability (BI), angular random walk (ARW), scale factor (SF), dynamic measurement range, bandwidth, and anti-interference, should be clarified according to the different application environments. Specifically, the two most important parameters for the inertial navigation applications are the BI and ARW. The BI represents the accuracy of the gyroscope for a long time, which reflects the change of the bias with time after the gyroscope is electrically stabilized, related to the flicker noise. And the ARW represents the accuracy of the gyroscope in a relatively short time, related to the thermo-mechanical white noise, which results in a zero-mean error with a standard deviation.

Besides, the SF, also named sensitivity, is the linear correlation coefficient between the output and input angular rate. A large SF can suppress the noise and interference to achieve a higher signal-to-noise ratio (SNR). Improving the mechanical quality factor can increase the SF, but it also results in a smaller bandwidth. Moreover, in general, a gyroscope with the proper dynamic measurement range (or full-scale range) is selected because the relative accuracy of a sensor is constant; theoretically the better ARW and larger SF will result in the smaller dynamic measurement range. That means that not all the performance indexes can be improved at the same time, and generally the researchers need to find a trade-off point based on different application requirements. On the other hand, although the gyroscope is a sensor that measures the angular rate and angular vibration, too much impact from the outside will cause it to fail. For example, one parameter named the shock range means the largest acceleration range bearable by the gyroscope.

According to the key parameters mentioned above, gyroscopes can be generally divided into three grades: rate-grade, tactical-grade, and inertial-grade, which correspond to low precision, medium precision, and high precision performances, respectively. Specifically, the rate-grade gyroscopes are mainly used in the consumer electronics, automobile navigation, and other occasions. And tactical-grade gyroscopes are mainly used in the aircraft navigation, attitude positioning, and other fields, which require both short-term and long-term accuracies. Moreover, inertial-grade gyroscopes are often used in the navigation, satellite positioning, scientific survey, and other fields, which require the ultra-high precision.

SECTION 1

MICROELECTROMECHANICAL (MEMS) GYROSCOPES

Modern technological progress depends on the development of microelectromechanical systems (MEMS), among which MEMS resonators occupy a special place. These compact and efficient devices play an important role in creating stable and precise electronic systems, ensuring their reliable operation in various fields.

The modern technology of microelectromechanical gyroscopes (MEMS gyroscopes) has opened up wide opportunities for improving inertial measurement systems, increasing their accuracy and efficiency.

In this section, we will take a closer look at the types of MEMS resonators, including oscillating and vibrating, their operating principles and practical applications. Exploring their structure, function and capabilities will allow us to gain a deeper understanding of these important components and their role in the current technological paradigm.

This paper will also provide an analysis of current achievements in the field of MEMS resonators, their advantages, disadvantages and prospects for further development. In particular, we will look at specific examples of MEMS resonators in various fields of engineering and technology, which will allow us to cover a wide range of capabilities of these devices. Particular attention will be paid to 2D and 3D resonators, manufacturers and manufacturing technologies that determine the quality and performance of these important components.

1.1. Definition of Microelectromechanical systems (MEMS)

MEMS, short for microelectromechanical systems, encompass devices merging interconnected mechanical and electrical components of micron size. These systems comprise mechanical elements, sensors, electronics, actuators, and microelectronic devices situated on a shared silicon substrate.

Among the functional components of MEMS, microsensors and microactuators stand out as particularly significant. Falling under the category of "transducers," these elements convert energy from one form to another. Microsensors typically translate measured mechanical signals into electrical ones.

The composition of MEMS includes components like microprocessors, microsensors, microactuators, data processing units, and elements for interfacing with external parts, as illustrated in Fig. 1.1.2.

In contrast to traditional mechatronic devices, MEMS often utilize the same mass production technologies employed for integrated circuits (ICs). Many commercial MEMS products are integrated and packaged with ICs. This fabrication approach enables the integration of microsensors for data collection and microactuators for converting energy into motion on a single substrate.

While MEMS offer low production costs per device, packaging poses a significant challenge. Each MEMS device must be packaged to safeguard electrical or optical circuits and other components from air and water contamination while still permitting interaction with the environment and adaptability to movement.

Typically, MEMS are divided into two types: sensors - measuring devices that translate certain physical influences into an electrical signal, and actuators (actuators) - systems that perform the opposite task, i.e. translate signals into certain actions [3].

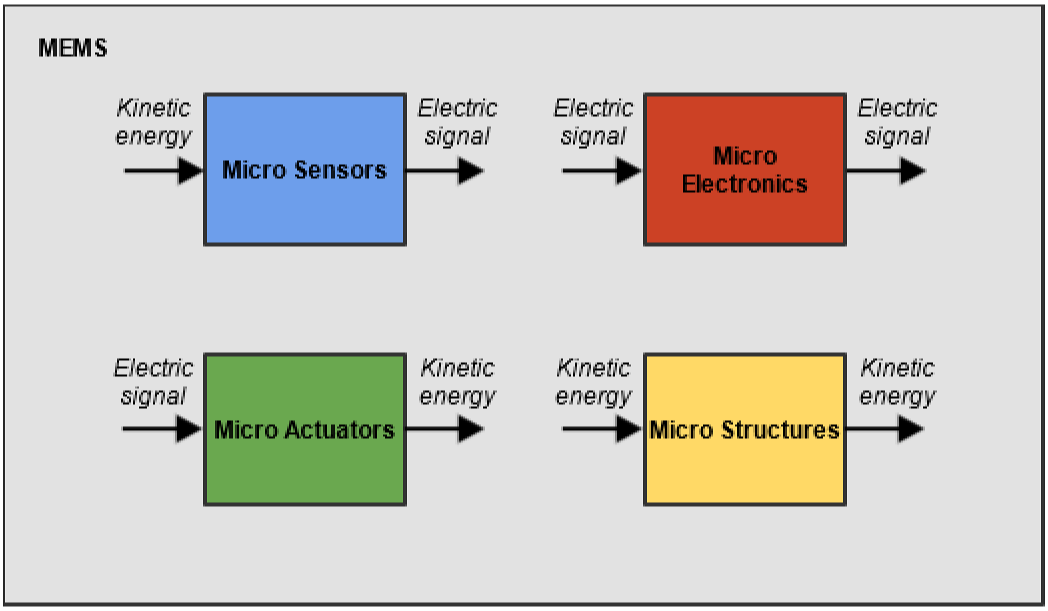

Fig. 1.1.2. MEMS structure

MEMS devices are typically fabricated on a silicon substrate using micromachining technology, similar to that of single-chip integrated circuits. Typical dimensions of micromechanical elements range from 1 micrometer to 100 micrometers, while the crystal dimensions of a MEMS chip range from 20 micrometers to one millimeter.

What are the uses of MEMS?

Microelectromechanical systems (MEMS) are used in various sensors, actuators, generators, energy sources, biochemical and biomedical systems and oscillators. Some examples of MEMS applications in engineering product design include [4]:

Sensors such as MEMS accelerometers, MEMS Microphones, MEMS gyroscopes, MEMS pressure sensors, MEMS tilt sensors and other types of MEMS resonant sensors [5][6].

Actuators such as MEMS switches, micro-pumps, micro-levers and micro-grippers.

Generators and energy sources such as MEMS vibration energy harvesters, MEMS fuel cells and MEMS radioisotope power generators.

Biochemical and biomedical systems such as MEMS biosensors, lab-on-chips, and MEMS air microfluidic and particulate sensors.

MEMS oscillators for accurate timekeeping and frequency control applications.

Advantages of MEMS:

- They are highly scalable in manufacturing, leading to significantly lower unit costs when produced in large quantities.
- MEMS sensors exhibit extremely high sensitivity, making them ideal for precise measurements.
- MEMS switches and actuators can operate at very high frequencies, enabling fast response times.
- MEMS devices consume very little power, making them efficient for battery-powered applications.
- They can be easily integrated with microelectronics to create embedded mechatronic systems, such as microphones.
- The scaling effects at microscopic levels allow for innovative designs and dynamic mechanisms not achievable at larger scales.

Disadvantages of MEMS:

- The research and development phase for new MEMS designs or devices can be very expensive.
- Setting up fabrication cleanrooms and foundry facilities incurs high upfront costs.
- Unit costs for fabrication and assembly can be prohibitive for low quantities, limiting their suitability for niche applications unless cost is not a concern.
- Testing equipment required to characterize MEMS quality and performance can also be costly [4].

1.2 What is the gyroscope?

Gyroscopes are devices that measure and maintain orientation using the principle of angular momentum. They are used in a wide range of applications, from navigation and aerospace to robotics and gaming. There are several types of gyroscopes, each with their own advantages and disadvantages.

Gyros come in a variety of shapes and sizes, depending on the specific application. Some of the most common types of gyroscopes include mechanical gyroscopes, fiber optic gyroscopes, and ring laser gyroscopes. Each type of gyroscope has its own unique strengths and weaknesses, and engineers and scientists choose the most appropriate type for their specific needs.

Gyroscopes find diverse applications across various industries. In aerospace and aviation, they play a crucial role in ensuring the stability and trajectory control of aircraft and spacecraft. Within robotics and automation, gyroscopes aid robots in preserving orientation and stability during task execution. In sports and gaming, gyroscopes enable precise control over movements in virtual reality and motion-controlled games. Additionally, gyroscopes contribute to navigation systems like compasses and GPS devices, assisting in accurate determination of location and directional orientation [7].

An array of gyroscopic types finds application across different domains, from aviation and navigation to robotics and stabilization systems. Alongside mechanical gyroscopes, fiber optic gyroscopes, and ring laser gyroscopes, other notable variants include hemispherical resonator gyroscopes (HRG) and microelectromechanical system (MEMS) gyroscopes.

Mechanical gyroscopes, among the earliest gyroscopic forms, have been in use for over a century. Operating on the principle of angular momentum, they offer simplicity and reliability. However, their bulk and weight may exceed those of alternative gyroscopic types.

Fiber-optic gyroscopes (FOGs) use the interference of light waves to measure angular velocity. They are highly accurate and rugged and are popular in aerospace and defense applications.

Ring laser gyroscopes (RLGs) use the interference of laser beams to measure angular velocity. They are highly accurate and reliable, and are used in a variety of industries, from navigation to geology.

Hemispherical resonator gyroscopes (HRGs) use the resonance of a vibrating hemisphere to measure angular velocity. They are small and lightweight and are well suited for use in MEMS and other applications where size and reliability are important.

Microelectromechanical system (MEMS) gyroscopes use microfabrication techniques to create miniature sensors. They have low power consumption and can be used in a wide range of applications, from consumer electronics to autonomous vehicles.

How a gyroscope works

It consists of a rotating rotor or disc mounted on a set of gimbals, which are rings that allow the rotor to rotate freely in any direction. The rotor stays in a fixed plane of rotation even when the rest of the gyroscope moves, due to a phenomenon known as gyroscopic precession. Gyroscopic precession is based on the conservation of angular momentum. When the gyroscope is set to rotate, it creates an axis of rotation around which the rotor rotates. As long as the axis of rotation is not disturbed, the rotor will continue to rotate in the same plane, even if the gyro tilts or turns in other directions. This is because any external forces acting on the gyro cause it to be trimmed, which means that the rotor's axis of rotation changes direction rather than orientation [8].

Advantages of gyroscopes:

- Stability: Gyroscopes maintain their orientation in space regardless of external forces, making them ideal for navigation systems.

- Accuracy: Gyroscopes are highly precise and can measure even the smallest changes in orientation, useful for precise instruments.
- Compactness: They can be very small and light, making them ideal for portable devices.
- Low power consumption: Gyroscopes require little energy, making them efficient for battery-powered devices.
- Versatility: They are used in a wide range of fields, from navigation to robotics and scientific research.

Disadvantages of gyroscopes:

- Power consumption: Constant power is needed for gyroscopes, which can be a drawback in certain conditions.
- Sensitivity to external factors: They can be affected by temperature, vibration, and electromagnetic interference.
- Drift: They may experience drift over time, leading to errors in measurements.
- Cost: High-precision gyroscopes can be expensive and inaccessible for some applications.
- Size and weight: Some types can be large and heavy, limiting their use in certain areas.

1.3. Introduction of MEMS-gyroscopes

The MEMS gyroscope (Fig. 1.3.1) is an inertial sensor, comprising a small device that measures angular velocity or rotation rate. It plays a crucial role in aerospace applications, unmanned aerial vehicles (UAVs), and various other fields. Additionally, it is utilized in navigation systems to detect changes in direction and measure pitch, roll, and yaw. Moreover, it finds applications in industries like oil extraction, mineral mining, providing solutions for north finding, pointing, and initial alignment, among others.

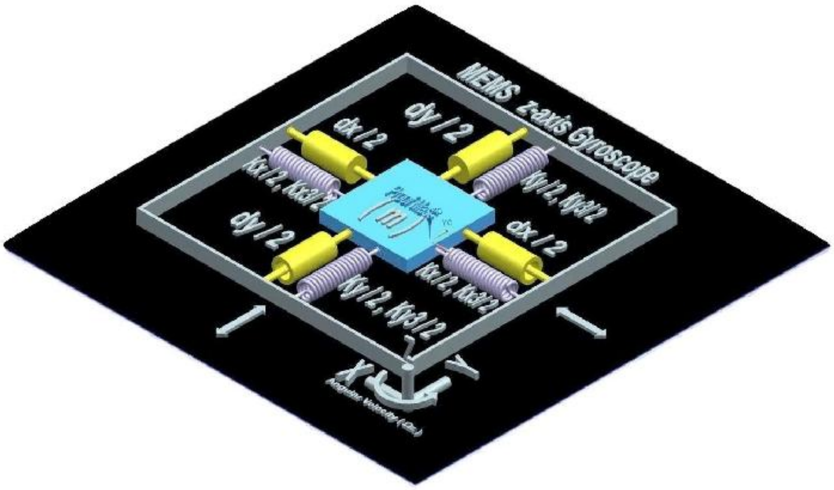

Fig. 1.3.1 Schematic showing MEMS gyroscope model

The principle of operation

MEMS gyroscopes exploit the Coriolis effect to gauge angular rate. This phenomenon manifests when an initially rotating object undergoes linear motion within a rotating reference frame. In this frame, its trajectory appears linear, but in an inertial frame, it deviates owing to external forces, notably the Coriolis force. This force, perpendicular to the object's motion, arises from its inertia in straight motion. Figure 1.3.2 illustrates the concept of the Coriolis effect.

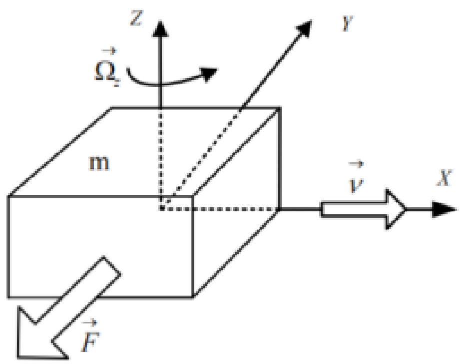

Fig. 1.3.2. Principle of Coriolis effect

If we consider the scenario depicted in Fig. 1.3.2, where object m moves uniformly along the X-axis with a velocity vv and simultaneously rotates around the Z-axis with an angular rate Ω_z, we can determine the Coriolis force acting on *m*.

The Coriolis force on mm in this situation is given by the formula:

$$\vec{F}_{Coriolis} = -2m\left(\overrightarrow{\Omega_z} \times \vec{v}\right),$$

where *m* represents the mass of the object;

Ω denotes the angular velocity vector ($\Omega = \Omega_z k$, where k is the unit vector along the Z-axis);

v signifies the velocity vector (v=vi, where i is the unit vector along the X-axis).

By plugging in these values into the formula, we can compute the Coriolis force acting on object m

Capacitive induction serves as the method for measuring displacement changes in MEMS gyroscopes induced by the Coriolis force. These gyroscopes comprise a vibrating block and a flexible spring. The crucial condition for the Coriolis force to be effective is the simultaneous rotation of the MEMS gyroscope around the Z-axis and the vibration of the vibrating block.

In motion, the capacitance detection sensor on the vibrating block facilitates energy transfer, resulting in fluctuations in electrochemical quantity. This mechanism allows for the transformation of the gyroscope's angular velocity into changes in capacitance, which are subsequently detected for measurement [9].

Characteristics of MEMS gyroscopes:

1. Small size, low weight, and low energy consumption.
2. Cost-effective for mass production.
3. High dynamic range, stability, and reliability.

4. Suitable for use in harsh mechanical environments.
5. Quick response time, ideal for fast-response systems.
6. Moderate precision, suitable for short-term applications or integration with other information systems.

Applications of MEMS gyroscopes:

1. Oil drilling: Used for north finding in logging tools and pointing in drilling equipment for accurate work.
2. Aerospace and drones: Initial alignment of UAV launch systems, precise attitude maintenance, navigation, and control.
3. Mining: Pointing and steering of advanced mining equipment in challenging underground environments.
4. Surveying: Orientation, positioning, and navigation in ground, sea, and air mapping systems.
5. Inertial platforms: Used for maintaining dynamic attitude datum and adjusting platform attitude and position.
6. Attitude balance: Indicating aircraft flying posture for pilot control and safety during flight.
7. Electronic devices: Consumer-grade MEMS gyroscopes in digital cameras for anti-shake function, mobile phone positioning, and gaming controls [10].

Various areas of application

The ER-MG2-50/100 and ER-MG2-300/400 MEMS gyroscopes (Fig. 1.3.3) represent a significant advancement over previous generations, addressing issues like size, mass, and cost. These new gyroscopes offer benefits such as compact size, low power consumption, affordability, robust overload resistance, large dynamic range, and integration capabilities. They can be seamlessly integrated into electronic, information, and intelligent control systems, resulting in reduced system volume and costs while significantly enhancing overall performance.

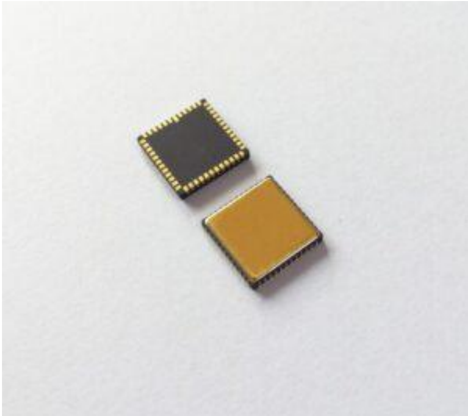

Fig. 1.3.3. The ER-MG2-50/100/ER-MG2-300/400 MEMS gyroscope

These advancements have opened up a wide array of applications in the modern military industry. The high-precision micromechanical gyroscope is poised to play a crucial role in missiles, aerospace, aviation, and other high-precision equipment where accuracy and stability are paramount. Moreover, these gyroscopes hold promise for modern unmanned navigation systems, satellite positioning navigation systems, information mapping, resource exploration, and other related fields due to their exceptional performance and versatility [11].

Let's consider photos of different MEMS gyroscopes (Fig. 1.3.4).

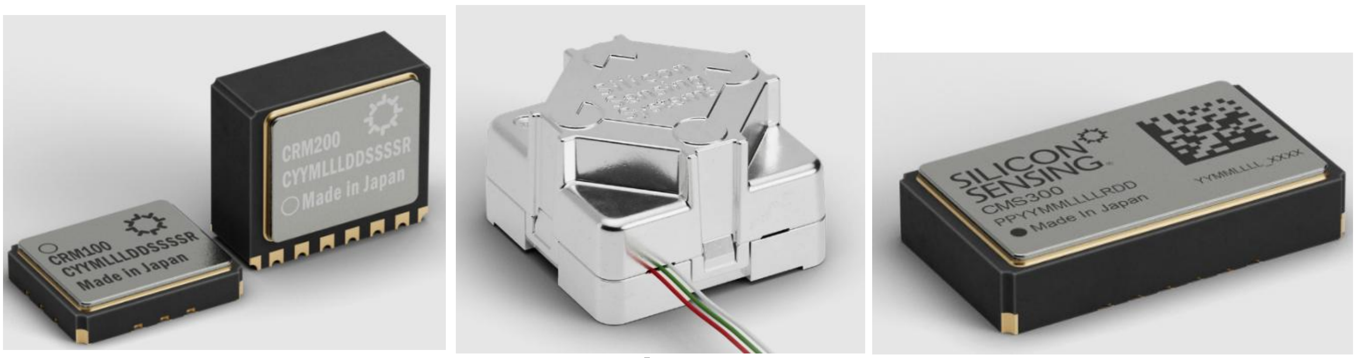

a *b* *c*

Fig. 1.3.4. Precision single-axis MEMS gyroscopes (Japan).
a – *CRM* PINPOINT, *b* – CRS43, *c* – CMS300 (IN-PLANE)

1.4. 2D MEMS resonators

2D MEMS resonators consist of tiny mechanical elements that oscillate within two dimensions, typically within a planar structure. Their operation relies on the principle of mechanical resonance, wherein they vibrate at specific frequencies when subjected to an external stimulus or force. These resonators often adopt a slim, flat design, taking shapes such as squares, circles, or rectangles, and are strategically positioned on a substrate to enable unrestricted oscillation.

Various vibration modes can be exhibited by these resonators, including bending and torsional modes, each associated with a unique resonant frequency. Materials like silicon, polymers, and piezoelectric substances such as lead zirconate titanate (PZT) are commonly utilized in constructing 2D MEMS resonators. The choice of material is influenced by factors such as mechanical properties and compatibility with manufacturing processes.

Performance Parameters of 2D MEMS Resonators

MEMS resonators are emerging as powerful alternatives to quartz resonators, especially in applications related to timing, frequency control, and resonant sensors. Understanding their key performance parameters is essential for optimizing their functionality and applicability.

- Resonant Frequency: The resonant frequency represents the natural vibration frequency of the resonator, determined by physical dimensions and material properties. It is critical for accurate timing and frequency referencing.
- Quality Factor (Q): The quality factor defines the energy dissipation rate and dynamic response of the resonator. Higher Q factors indicate lower energy loss and improved signal-to-noise ratio [12].

- Frequency Accuracy: Frequency accuracy measures the closeness of the actual frequency to the desired frequency. This parameter is crucial for precise clock synchronization and communication systems.
- Electromechanical Coupling Coefficient: This coefficient quantifies energy transfer efficiency between electrical and mechanical domains. Higher coupling coefficients enhance overall resonator performance.
- Motional Resistance: Motional resistance reflects energy dissipation due to mechanical losses. Lower motional resistance correlates with improved resonator efficiency.
- Temperature Stability: Temperature stability addresses frequency shifts with temperature variations. Achieving stable performance across temperature ranges is vital for consistent functionality.

The integration of 2D materials, MEMS technology, and Inertial Measurement Units (IMUs) offers promising avenues for precision sensing and navigation applications. This convergence opens up exciting possibilities for enhancing performance and reliability in various technological domains [13].

Key Characteristics and Properties:

1. High-Frequency Operation: 2D MEMS resonators excel in operating at exceptionally high frequencies, facilitating accurate measurements and signal processing.

2. Miniaturization: Their thin profile and compact size enable seamless integration into small-scale devices.

3. Sensitivity: These resonators exhibit a responsive nature to external influences, enabling precise detection of changes such as mass, pressure, or temperature variations.

4. Customizable Properties: Researchers can tailor the resonators' properties by adjusting size and deformation, making them adaptable to specific applications.

Applications:

1. Timing Devices and Frequency Control: 2D MEMS resonators are crucial components in timing devices, oscillators, and frequency control systems, ensuring the generation of stable clock signals in electronic devices.
2. MEMS-Based Sensors: They play a vital role in MEMS-based sensors used for measuring parameters like mass, pressure, and acceleration.
3. Radio Frequency Systems: These resonators are employed in radio frequency systems for signal processing and filtering, enhancing the functionality of communication systems.
4. Sensors for Environmental Monitoring and Industrial Processes: They contribute to detecting changes in mass, gas concentration, and temperature, making them valuable for environmental monitoring, healthcare, and industrial processes.
5. Communication Devices: Their high-frequency operation qualifies them for use in filters, oscillators, and frequency references within communication devices.
6. Quantum Technologies: Researchers are exploring the potential of 2D MEMS resonators in quantum sensors and quantum communication applications.

Manufacturing Techniques

The dry transfer method stands out from wet processes in the production of 2D material resonators on MEMS actuators. This method prioritizes stability and reliability during fabrication. Platinum Clamping: A platinum layer is applied onto the 2D membrane to securely anchor it within the MEMS structure. This measure prevents slippage and enhances stability.

The manufacturing process for 2D MEMS resonators integrates sophisticated microfabrication technologies like photolithography, etching, deposition, and bonding.

These methods enable meticulous control over dimensions and properties, crucial for achieving targeted resonant frequencies and desired performance attributes.

In essence, 2D MEMS resonators present compact, energy-efficient solutions with precise frequency management, rendering them versatile components across electronics, sensor applications, and communication technologies.

Manufacturers of 2D MEMS Resonators

1. **SiTime XCalibur™ Active Resonators:**

Designed to replace 4-pin SMD crystal resonators. Provide stability, reliability, and ease of design. Eliminate the need for tuning capacitors. Can drive two clock inputs.

2. **TempFlat MEMS™ Embedded MEMS Resonators:**

Smaller in size (up to 85% smaller than quartz crystal resonators). Can be integrated into standard IC packages, SIPs, or modules. Offer better reliability, higher performance, and environmental resilience [14].

An Inertial Measurement Unit (IMU) is a device that measures and reports a body's specific force, angular rate, and sometimes the magnetic field surrounding the body, using a combination of accelerometers, gyroscopes, and magnetometers. IMUs are crucial components in applications such as navigation, robotics, and motion tracking [15].

In the context of 2D MEMS resonators, an IMU could be designed using 2D MEMS resonators as both accelerometers and gyroscopes. Here's how it could work:

1. **Acceleration Measurement**:
   - The 2D MEMS resonator is designed to act as an accelerometer. When the IMU experiences acceleration, the resonator's mass distribution shifts, causing it to vibrate in a particular mode.
   - The frequency of this vibration, which changes due to the acceleration, is measured to determine the magnitude and direction of the acceleration.

2. **Angular Rate Measurement**:
    - To measure angular rate (angular velocity), the 2D MEMS resonator is utilized as a gyroscope. When the IMU rotates, the Coriolis effect causes the resonator to experience a force perpendicular to its plane of vibration.
    - This force induces a secondary vibration in the resonator, the frequency of which is proportional to the angular rate of rotation. By measuring this frequency change, the IMU determines the rotation rate.
3. **Integration**:
    - By combining the data from the accelerometer (for linear motion) and gyroscope (for angular motion), the IMU can provide information about the device's orientation, velocity, and displacement over time.
    - Algorithms such as sensor fusion (e.g., Kalman filtering) are often used to integrate and filter the sensor data, improving accuracy and reducing noise and drift.
4. **Calibration and Compensation**:
    - Calibrating the IMU involves compensating for factors like sensor biases, temperature variations, and mechanical imperfections in the resonators to ensure accurate and reliable measurements.
    - Advanced IMUs may also include magnetometers to account for magnetic field influences and provide additional orientation information (e.g., heading).

In summary, an IMU based on 2D MEMS resonators can provide precise measurements of acceleration and angular rate, enabling accurate motion tracking, orientation estimation, and navigation in various applications [16][17].

1.5. 3D MEMS resonators

3D MEMS resonators represent micro-electro-mechanical systems that engage in three-dimensional vibrations, expanding the scope of available vibration modes and applications in contrast to their 2D equivalents. These resonators are commonly manufactured using sophisticated microfabrication methodologies and have the capacity to manifest diverse vibration modes including bending, torsional, longitudinal, and radial modes. They find utility in an array of applications such as sensors, actuators, frequency references, biomedical devices, and various others, particularly in scenarios necessitating accurate multi-axis sensing, actuation, or frequency modulation.

Fig. 1.5.1 shows of the ULE TSG/fused-quartz fabricated 3D wineglass and spherical shells, including hemispheres with hollow and solid stems of different diameters, are displayed with permission from Elsevier.

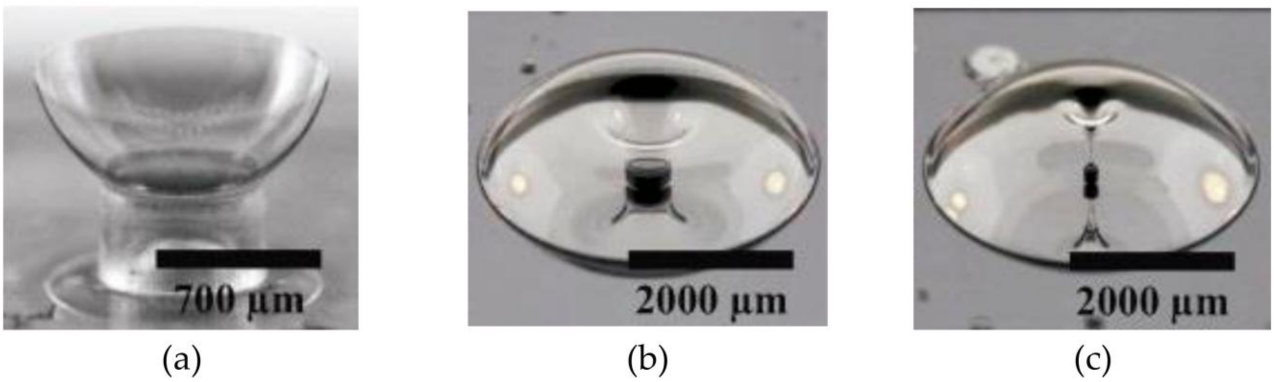

Fig. 1.5.1. ULE TSG/fused-quartz fabricated 3D wineglass and spherical shells with permission from Elsevier. (a) a hemisphere with a hollow stem, (b) a hemisphere with a

solid stem of 500 µm diameter, and (c) a hemisphere with a solid stem of 60 µm diameter

Fig. 1.5.2 shows the final fabricated hemispheres with integrated electrodes integrated electrodes and the frequency response showing the subgigahertz frequency distribution of the resonator [18].

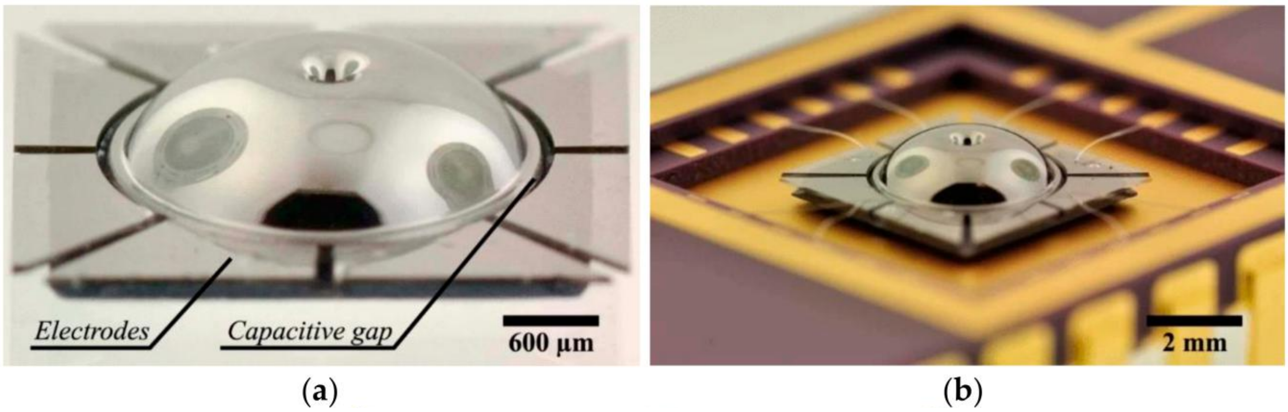

Fig, 1.5.2. Metallised micro-glass structure featuring integrated electrodes with a diameter of 4 mm and a thickness of 50 µm. (a) metallised micro-glass structure with integrated electrodes. (b) the packed and wire-wrapped device

Performance Parameters of 3D MEMS Resonators

Complexity of Mode Shapes: In contrast to the relatively straightforward mode shapes observed in 2D resonators, 3D MEMS resonators exhibit more intricate and spatially complex mode shapes, owing to the increased degrees of freedom in three dimensions.

Utilization of Higher-Order Modes: While 2D resonators mainly operate in their fundamental mode, 3D resonators can effectively utilize higher-order modes, providing a wider range of frequency options that can be advantageous for specific applications.

Impact of Nonlinear Effects: The structural complexity of 3D resonators leads to more pronounced nonlinear effects, which can significantly influence frequency stability, energy dissipation, and dynamic behavior.

Intermodal Coupling: 3D resonators often demonstrate stronger coupling between different vibrational modes, resulting in phenomena like mode mixing and frequency splitting that add complexity to their behavior.

Manufacturing Complexity: Fabricating 3D MEMS resonators involves intricate processes such as deep etching, wafer bonding, and sacrificial layer removal, presenting distinct challenges compared to the planar fabrication methods used for 2D resonators.

Consideration of Anisotropic Material Properties: In 3D structures, material properties like Young's modulus, Poisson's ratio, and thermal expansion coefficients can vary significantly along different axes, necessitating careful consideration of anisotropy for accurate modeling and design.

Exploration of Topology Optimization: The three-dimensional nature of MEMS resonators allows for greater freedom in exploring topology optimization, enabling designers to experiment with novel geometries such as curved surfaces, hemispherical shells, or intricate lattice structures to enhance performance.

Integration Capabilities: 3D resonators can be seamlessly integrated with other MEMS/NEMS components such as sensors, actuators, and microfluidic channels, facilitating the development of multifunctional devices with enhanced capabilities [19].

Example of 3D Multi-frequency MEMS resonator concept

The resonator is made of single-crystal silicon, and we utilized the material characteristics mentioned in the preceding section. We assume that the structural silicon is stress-free (σ=0). The anchor is a rectangular prism measuring 2 by 2 micrometers (thickness: 50 nanometers), while the resonator has a thickness of 400 nanometers. Our simulation employed a rectangular mesh (refer to Fig. 1.5.3) with enhanced refinement around the anchor region to accurately capture the central nodal point area. Details of the simulation conditions are provided in Table 1 below [20].

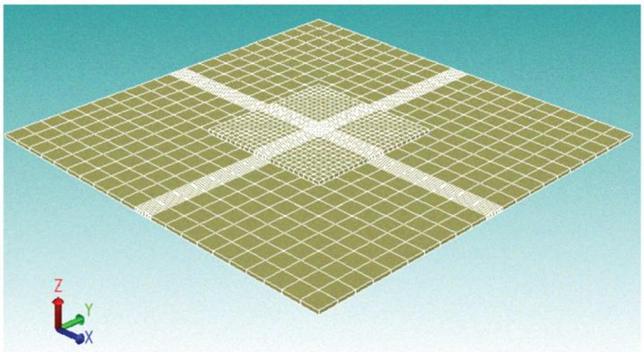

Fig. 1.5.3. 3D resonator mesh with anchor area refinement

Table 1

Simulation conditions

Parameter	**Value**
Material	Single-crystal silicon
Young's Modulus (E)	180 GPa
Density (ρ)	2330 kg/m³
Poisson's Coefficient (ν)	0.29
Intrinsic Stress (σ)	0 MPa
Anchor Dimensions	2x2x0.08 μm³
Plate Thickness (h)	0.04 μm
Mesh	Parallelepiped (10 elements/segment)

Manufacturers of 3D MEMS resonators

1. **Silicon Sensing Systems Ltd.**: This company specializes in MEMS-based gyroscopes and accelerometers, including 3D MEMS resonators for inertial sensing applications.

2. **Qualtre Inc.**: Qualtre focuses on high-performance MEMS sensors, including 3D MEMS resonators used in inertial measurement units (IMUs) and motion sensing applications.
3. **Vesper Technologies**: Vesper develops advanced MEMS microphones and sensors, including 3D MEMS resonators for acoustic sensing and other applications.
4. **STMicroelectronics**: STMicroelectronics is a major semiconductor manufacturer that produces a wide range of MEMS sensors and actuators, including 3D MEMS resonators for automotive, industrial, and consumer electronics applications.
5. **TDK Corporation**: TDK offers MEMS-based sensor solutions, including 3D MEMS resonators used in inertial navigation systems, vibration monitoring, and industrial automation.
6. **Bosch Sensortec**: Bosch is known for its MEMS sensor technologies, including 3D MEMS resonators used in automotive applications, consumer electronics, and IoT devices.

These manufacturers often integrate 3D MEMS resonators into complete sensor systems or offer them as standalone components for various applications in sectors such as automotive, aerospace, healthcare, and consumer electronics [14].

1.6. Conclusion

After reviewing and analyzing microelectromechanical gyroscopes (MEMS gyroscopes), several important conclusions can be drawn. Firstly, MEMS gyroscopes are important components in modern navigation, automation and industrial control systems due to their properties of accurate angular velocity measurement and compactness.

Further, an analysis of the principles of operation and applications of MEMS gyroscopes has shown their versatility in various fields, from aviation to medicine and the automotive industry. Important parameters of their efficiency are measurement accuracy, speed and resistance to external factors.

It is also worth noting the role of 2D and 3D MEMS resonators in the functioning of MEMS gyroscopes, as they determine their sensitivity and resistance to internal and external influences.

The main differences between 2D and 3D MEMS resonators lie in their structural design, vibration modes, and applications. Here's a comparison:

1. **Structural Design**:

- **2D MEMS Resonators**: These resonators have a flat, planar structure, often resembling squares, circles, or rectangles. They vibrate primarily in a single plane.
- **3D MEMS Resonators**: In contrast, 3D MEMS resonators have a three-dimensional structure, such as cubes, spheres, or complex geometries. They can vibrate in multiple modes and directions, offering additional degrees of freedom.

2. **Vibration Modes**:

- **2D MEMS Resonators**: Typically exhibit vibration modes like bending (flexural) and twisting (torsional) in a single plane.
- **3D MEMS Resonators**: Can exhibit a wider range of vibration modes, including bending, torsional, longitudinal, radial, and others, due to their three-dimensional structure.

3. **Applications**:

- **2D MEMS Resonators**: Commonly used in applications requiring single-axis or planar sensing, such as accelerometers and gyroscopes in smartphones, automotive systems, and navigation devices.
- **3D MEMS Resonators**: Suitable for multi-axis sensing, complex motion tracking, inertial navigation systems, vibration analysis, and applications requiring precise control in multiple directions.

4. **Sensing Capability**:

- **2D MEMS Resonators**: Primarily used for sensing motion or forces along a single axis or plane.
- **3D MEMS Resonators**: Capable of sensing motion, forces, and vibrations in multiple axes or directions simultaneously, offering more comprehensive data for analysis.

5. **Fabrication Complexity**:

- **2D MEMS Resonators**: Generally simpler to fabricate due to their planar structure, using techniques like surface micromachining or bulk micromachining.
- **3D MEMS Resonators**: More complex to fabricate due to their three-dimensional nature, often requiring advanced techniques such as deep reactive ion etching (DRIE) and complex layer deposition processes.

6. **Versatility**:

- **2D MEMS Resonators**: Well-suited for applications where motion or forces occur predominantly in a single plane or axis.
- **3D MEMS Resonators**: Provide versatility for applications requiring motion or forces in multiple directions, enabling more comprehensive and accurate sensing and control.

In summary, while both 2D and 3D MEMS resonators are important in the field of micro-electro-mechanical systems, their structural differences lead to distinct capabilities and suitability for different applications, with 3D resonators offering enhanced multi-axis sensing and control capabilities [21].

In general, the first section of the work allowed us to gain a deeper understanding of the essence and significance of MEMS gyroscopes in the modern technological industry, as well as to identify key aspects of their functioning and application for further research and development.

SECTION 2

MEMS GYROSCOPES MODES OF OPERATION

2.1. Understanding the relevance of MEMS gyroscope research

Gyroscopes are important devices for measuring rotational motion and stabilizing systems. In recent years, microelectromechanical systems (MEMS) gyroscopes have gained popularity due to their compactness, low cost, and high sensitivity.

As we delve into the intricacies of MEMS gyroscopes, it becomes apparent that their operating modes, errors caused by manufacturing imperfections, and the phenomenon of periodic drift are not just technical details, but rather the essence of their functionality and reliability.

Understanding the operating modes of MEMS gyroscopes, namely velocity measurement, velocity integration and differential modes, reveals the essence of how these miniature wonders capture and interpret rotational motion. Each mode has unique characteristics and applications, forming the foundation on which precision navigation systems, stabilization platforms and motion tracking devices are built.

Understanding the inherent errors in MEMS gyroscopes due to manufacturing imperfections opens up an area where accuracy meets practical challenges. These imperfections, ranging from sensor misalignment to material mismatches, highlight the need for careful calibration and error correction methodologies to obtain reliable data in real-world applications.

In addition, understanding the intricacies of MEMS resonators, including their Q-factor and frequency mismatch, provides insight into the physics behind their resonance, as well as the implications for the accuracy and stability of gyroscopic measurements Q-factor, a measure of energy dissipation in resonant systems, and frequency mismatch highlight the nuances that affect the performance and accuracy of MEMS gyroscopes.

An important aspect of MEMS gyroscopes is the understanding of periodic drift, especially in rate-integrating gyroscopes. This phenomenon, which is influenced by environmental factors, aging effects, and operating conditions, poses challenges to maintaining long-term accuracy and reliability, requiring advanced compensation techniques and calibration methodologies.

Finally, delving into the block diagrams of rate-integrated gyroscopes reveals the complex interplay of sensor elements, signal processing circuits, and feedback mechanisms that enable accurate measurement and interpretation of rotational motion.

In essence, learning about MEMS gyroscopes encompasses much more than technical descriptions; it shows an understanding of scientific research, engineering ingenuity, and practical challenges.

2.2. Description of operating mode types

At the moment, there are three known modes of operation of vibration MEMS gyroscopes: rate, rate-integrating and differential modes of operation

Compensation mode (Rate mode)

In this mode, the objective is to stabilize the standing wave within the vibration structure at one of its resonant frequencies. When rotation occurs, it induces a Coriolis force that excites a secondary standing wave. This secondary wave is compensated by negative feedback, effectively counteracting the Coriolis force. This compensation allows the standing wave to be maintained near the excitation electrode with a feedback signal that is proportional to the angular velocity.

The rate gyro, as depicted in Fig. 2.2.1, differs only by incorporating a spring system that acts as an additional restraint on the rotational motion of the frame. This instrument is designed to measure the absolute angular velocity of a body and is widely utilized for generating stabilizing signals within vehicle navigation systems. It typically provides a measurement resolution of 0.01 degrees/s, and it can accurately measure rotation rates of up to 50 degrees/s.

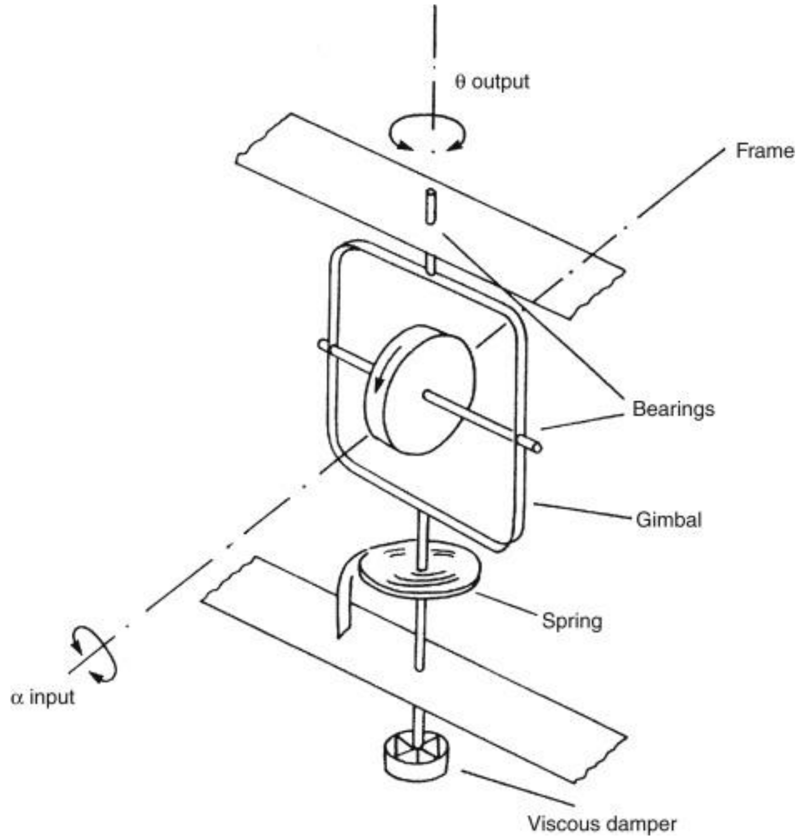

Fig. 2.2.1. Rate gyroscope

The angular velocity, α, of the body is related to the angular deflection of the gyroscope, θ, by the equation:

$$\frac{\theta}{\alpha}(D) = \frac{H}{MD^2 + \beta D + K}, \#(2.1)$$

where H represents the angular momentum of the spinning wheel;

M is the moment of inertia of the system;

β is the viscous damping coefficient;

K is the spring constant;

D is the D-operator.

This equation (2.1) is a second-order differential equation, indicating that the device's response follows second-order instrument characteristics. Therefore, careful design of the instrument is necessary to ensure that the output response is neither oscillatory nor excessively slow in reaching a final reading. To aid in the design process, eq. (2.1) can be reformulated as follows:

$$\frac{\theta}{\alpha}(D) = \frac{K^{'}}{D^2/\omega^2 + 2\xi D/\omega + 1},$$

where $K' = H/K$

$\omega = \sqrt{K/M};$

$\xi = \frac{\beta}{2\sqrt{K/M}}.$

The static sensitivity of the instrument, K′, is maximized by using a high-speed motor to increase H. Reducing the spring constant K further enhances sensitivity, but caution is needed as excessively low K values decrease the resonant frequency ω of the instrument. The damping coefficient β is typically selected to achieve a damping ratio ξ close to 0.7 [22].

Rotation Angle Measurement Mode (Rate-integrating Mode)

In the mode of operation of rate-integrating gyroscopes (RIGs), controlled angular motion about one of the axes of symmetry induces a specific form of oscillation in the shape of a standing wave. The Bryan effect influences this phenomenon, causing the angular velocity of the standing wave to differ from the external angular velocity of rotation. This disparity provides valuable insights into the inertial properties of a moving object. Typically, RIG sensing elements have a hemisphere shape, and to induce vibrations, they employ a series of electrodes subjected to periodic voltages. In such systems, parametric resonance effects can occur due to the periodic nature of the excitation force.

In this scenario, the Coriolis force remains uncompensated, but gyroscope errors are mitigated by compensating only the quadrature signal. Under the influence of the Coriolis force, the standing wave rotates relative to the vibrating structure, with the rotation angle being proportional to the gyroscope's angle relative to the inertial coordinate system. Bryan's coefficient reflects this proportionality between the gyro angle and the rotation angle of the standing wave, illustrating how Coriolis forces contribute to converting vibration energy from primary to secondary form.

The integrating gyroscope, which determines rotation angle by velocity integration, offers numerous advantages such as temperature independence, high linearity, wide operating range, and the use of a degenerate resonator where both rotation modes become eigenmodes.

Linear oscillation direction (the phase difference between independently controlled clockwise and counterclockwise oscillations) is utilized for rotation detection, akin to a Foucault pendulum. However, tuning the frequency and/or Q-factor eliminates degeneracy by combining clockwise and counterclockwise modes. Cross-coupling between these modes introduces interference, disrupting the oscillation direction.

For rate-integrating gyroscopes, the structure comprises oscillations that can develop along orthogonal axes, as depicted in Fig. 2.2.2. The Coriolis force transfers energy between these axes and alters their relative amplitudes. The amplitude ratio tracks the total rotation angle, which repeats every 2π, with a geometry-dependent scale factor of approximately 0.3 for ring or cylindrical gyros.

The control system must provide oscillations along the two axes without affecting the relative amplitudes. The quadrature component error signal is caused by damping and frequency tuning or anisotropy of the device. This error signal needs to be compensated for, otherwise the orientation of the oscillation nodes in the gyroscope will not be able to precess freely during rotation [24].

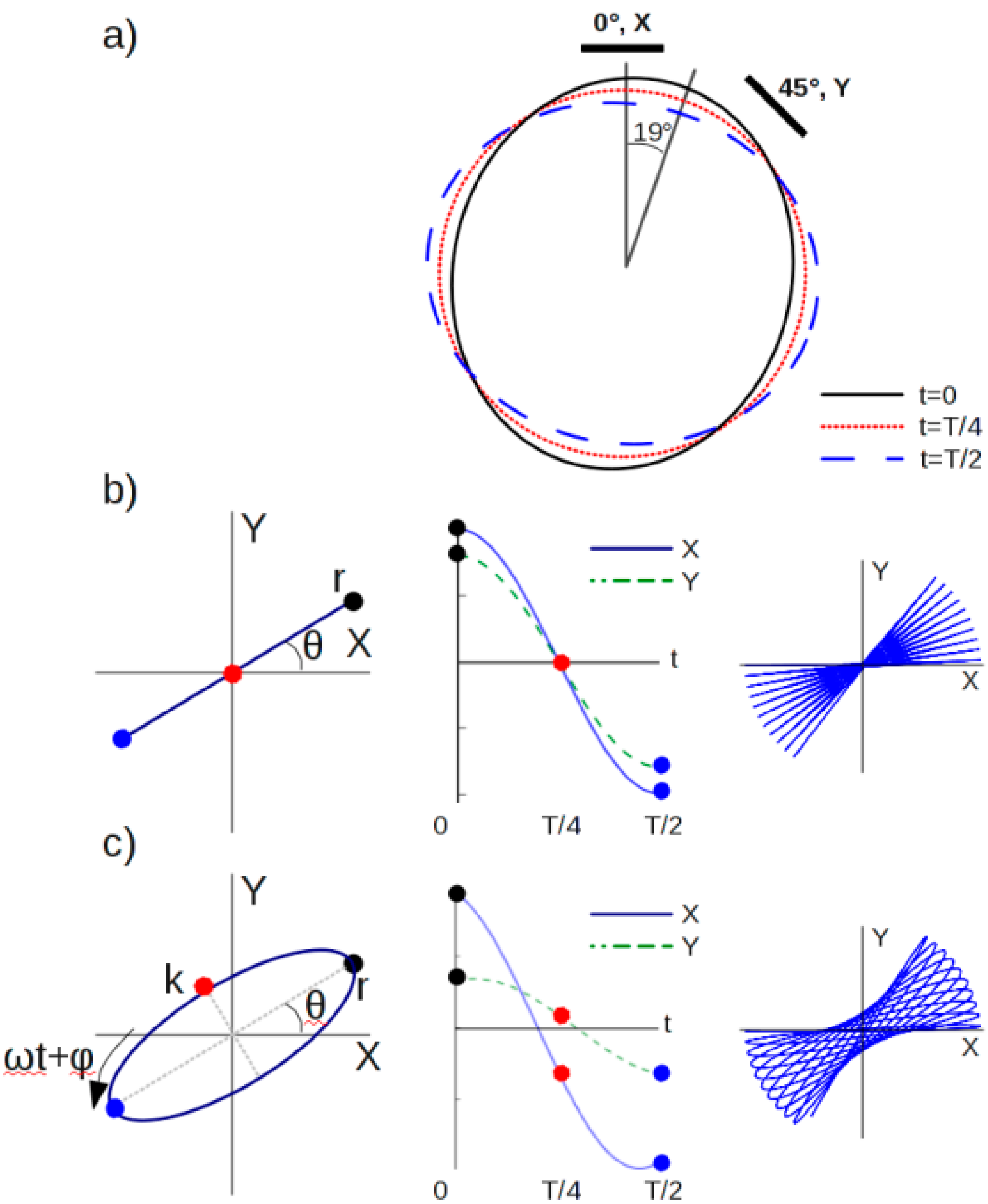

Fig. 2.2.2. a) Rate integrating MEMS gyroscopes with the standing wave rotated 19 from the X axis. b) The projection of this standing wave onto the X-Y axes, the corresponding output signal, and how the projection changes under continued rotation. c) Projection for a non-ideal gyroscope with significant quadrature error

Differential Mode of Operation

In the differential mode of operation, the standing wave is situated between electrodes using two excitation signals along the X and Y axes, positioned at a 45° angle. This setup creates two measurement channels, X and Y, each producing a signal proportional to the angular velocity with opposite signs, +Ω and -Ω. The resultant angular velocity can be derived by subtracting the signals from the measurement channels or employing redundancy in measurements of the same angular velocity. Diametrically opposite electrodes are short-circuited to diminish uncompensated torques from the drive electrodes and enhance signals from the sensing electrodes.

In this configuration (refer to Fig. 2.2.3), the ω_1 axis represents the axis of maximum resonator stiffness, while the τ_1 axis denotes the axis of minimum attenuation, corresponding to the maximum quality factor of the resonator. Positioned at an angle of θ_ω relative to the direction of standing wave oscillations, the τ_1 axis signifies the minimum damping axis, indicating the axis of maximum quality factor of the resonator. This axis is angled at θ_τ to the direction of oscillations of the standing wave. The orientation of the standing wave oscillations relative to the X drive electrode is designated as the zero position, angled at θ.

Utilizing a standing wave disposition between electrodes, the differential MEMS gyroscope generates two measurement channels with opposite-signed angle rates. This setup results in periodic dependence of scale factors and biases on the angular disposition of the standing wave, occurring with a period of π radians.

The integration of an additional operating mode alongside the angular and integrated modes enhances the versatility of the gyroscope. The differential mode of operation exhibits greater resilience to external disturbances like shock and vibration, effectively compensating for disturbances that affect both measurement channels simultaneously.

Thus, the control system that keeps the standing wave between the electrodes implements a differential mode of operation for the MEMS gyroscope. This mode allows for efficient measurement of angular velocity using a standing wave and provides greater sensitivity to changes in oscillation velocity [25].

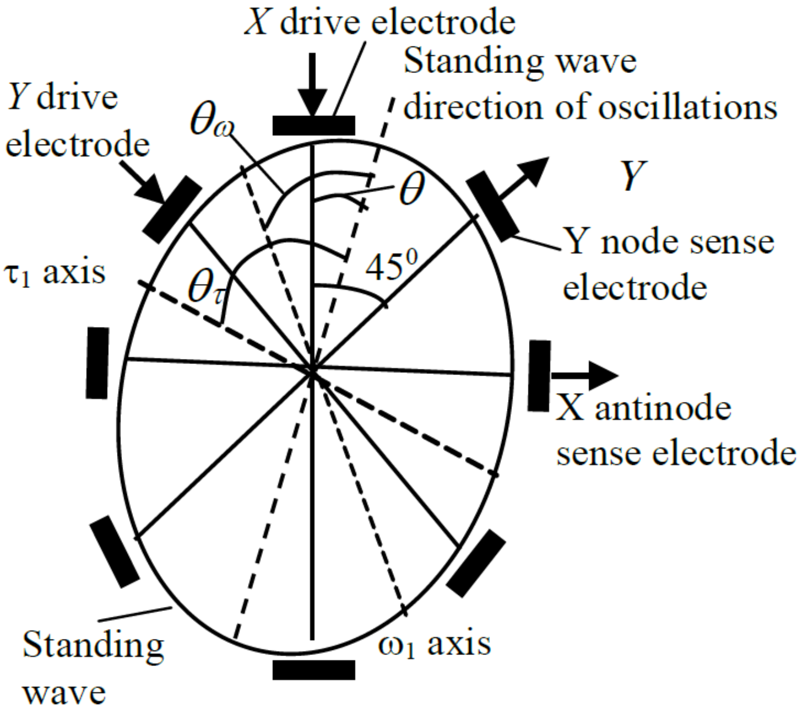

Fig. 2.2.3. Standing wave disposition for differential MEMS gyro

Absolutely, these modes play a pivotal role in accurately measuring angular velocity and guaranteeing stability and reliability across various applications. The differential gyro mode, in particular, provides additional capabilities to compensate for both internal and external destabilizing factors in angular velocity measurement. By effectively suppressing disturbances and enhancing measurement stability, the differential mode contributes significantly to the overall accuracy and robustness of gyroscopic systems.

MEMS gyroscopes are used in various operating modes (Table 2), each with its own characteristics and applications:

1. Angular velocity mode (rate mode): This mode is used to measure the angular velocity of an object. It is commonly used in stabilization and navigation systems, for

example, in automotive safety systems to determine vehicle movement and activate airbags in the event of a collision.

2. Rate-integrating mode: In this mode, the gyroscope accumulates angular velocity over time to detect changes in object orientation. This is useful in inertial navigation systems where it is necessary to accurately track the position of an object in space, such as in underwater vehicles or spacecraft.

3. Differential mode: It can be used in conditions where it is necessary to minimize the influence of vibrations and other external factors that can affect the accuracy of measurements, for example, in industrial robots or high-precision equipment.

The advantages of each mode depend on the specific application. Angular velocity mode provides a fast response to changes, making it ideal for systems that require an immediate response. Integrating mode provides more accurate position change data, which is important for long-term navigation tasks. Differential mode is distinguished by its ability to effectively suppress external disturbances, making it the choice for applications where high measurement stability is important.

Table 2

Advantages and disadvantages of gyroscope modes of operation [26]

Advantages		
Rate	Rate Integrating	Differential
• Low noise	• High dynamic range	• Higher resistivity to external disturbances
• Standing wave control simplicity	• High bandwidth	• Effective on-line compensation for the frequency mismatch

• Easy to calibrate resonator’s imperfections	• High stability of scale factor	• Possibility to online bias compensation
Disadvantages		
• Higher sensitivity to external disturbances	• Higher sensitivity to resonator’s imperfections	• Limited bandwidth
• Lower scale factor temperature stability	• Higher noise especially when measuring small angle rate	• Lower scale factor temperature stability

2.3. MEMS gyros errors due to manufacturing imperfection

Technological manufacturing errors and material non-uniformity are the main causes of errors in vibratory angular rate sensors (VARS). The most significant impact on VARS errors comes from the non-uniform mass distribution along the spatial coordinates of the resonator.

1. Deviations from the specified geometrical parameters: Technological errors in resonator manufacturing can include deviations from planned geometrical parameters such as dimensions, shape, surface characteristics and other parameters. This can be due to inaccuracies in the manufacturing processes, such as the accuracy of the machines used to process the materials, or changes that occur during the various stages of production.

2. Inaccuracies in mass and mass distribution: This category of errors refers to uneven mass distribution in the resonator or inaccuracies in mass measurements. For example, uneven material distribution can lead to changes in the vibration characteristics of the resonator and affect the accuracy of the measurements it makes.

3. Alignment and installation errors: This includes errors that can occur during the mounting process of the resonators in the gyroscope. For example, improper alignment

of the resonators can lead to a change in the center of mass of the system, which can affect its stability and performance. Mounting errors can also lead to mechanical stresses that affect the durability and reliability of the gyro.

4. Temperature errors: The manufacturing processes used in the production of resonators can be sensitive to changes in temperature conditions. For example, the thermal expansion of materials at high temperatures can lead to changes in their geometric and mechanical properties, which affects the resonator's performance.

5. Errors due to equipment wear: The equipment used to manufacture resonators can wear out, which can lead to changes in manufacturing quality. For example, tooling wear or inaccuracies in machine operation can affect the accuracy and quality of manufacturing processes, which affects gyroscope performance.

To minimize technological errors in the production of resonators, it is important to use high-precision equipment, carry out regular calibration and maintenance of the equipment, and apply thorough quality control at all stages of production.

For instance, for resonators that are thin spatial shells (rotational bodies), this non-uniformity arises from differences in shell thickness along the circumferential coordinate of the resonator. Fourier analysis shows that the difference in shell thickness (e.g., hemispherical, cylindrical, or ring-shaped) along the circumferential coordinate has the greatest impact on VARS error for the second mode of vibration ($n = 2$), where there are four nodes and antinodes along the perimeter of the resonator. This occurs due to the fourth harmonic of mass imbalance, which results in the splitting of the resonator's natural frequency into two frequencies. The maximum frequency splitting in this case can be estimated using the formula $\Delta\omega = \varepsilon\omega^2/2$, where ε relates to the defect magnitude at the fourth harmonic.

Fig. 2.3.1 depicts a simple distribution of shell thickness with a significant component at the 4th harmonic, where the thickness of the shell is greater at four equally spaced points compared to others. Shells typically smooth out local rigidities (or elasticities) through thickness variations. The primary contribution comes from the fourth harmonic of mass variation. Therefore, if a standing wave is located at nodes along a solid axis (see Fig. 2.3.1), and the resonator is considered as a second-order linear oscillatory system with approximately equal stiffness coefficients but slightly different weights, then the resonant frequency of the wave, whose antinodes are along the dashed axis, is slightly lower than the frequency of the second mode $n = 2$, when the antinodes are along the solid axis. The presence of two different normal mode frequencies results in the standing wave being located somewhere between the normal axes, as indicated in Fig. 2.3.1, where the angle is 45° for $n = 2$.

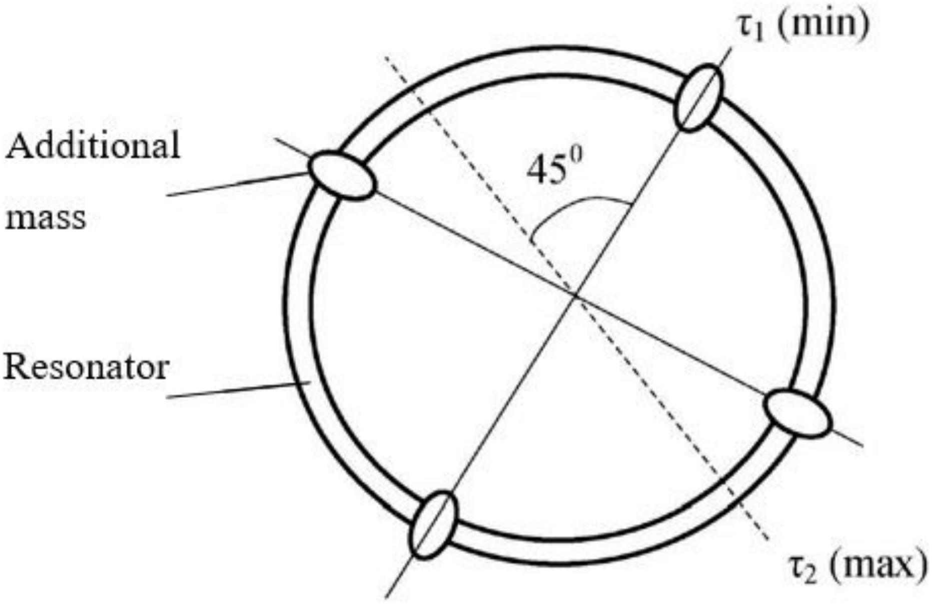

Fig. 2.3.1. Fourth harmonic of the mass distribution

To determine the resulting wave motion with an arbitrary location of the standing wave void, it is necessary to decompose the wave oscillations into components along the normal axes. Since these components oscillate at different frequencies, it should be noted that the composite standing wave ceases to be a standing wave as a traveling wave component develops. This is due to the fact that a quadrature component of the secondary wave is formed, whose void points coincide with the nodes of the primary wave, which oscillates with a quadrature phase relative to the primary wave, i.e. at a phase angle of 90°. In this case, the so-called standing wave drift appears, the velocity of which is determined by the following formula:

$$\dot{\theta} = \frac{1}{8} (\Delta\omega)^2 \cdot \ tsin4\varphi_0,$$

where φ_0 is the angle between the direction of oscillation and one of the resonator's natural axes (for example, the axis with the minimum oscillation frequency);

$\Delta\omega = \omega_{21} - \omega_{22}$ is the resonator natural frequency split.

When the direction of oscillation coincides with one of the resonator's natural axes, it can be seen that at $\varphi_0 = 0$, $\pi/4$, but there is no wave drift, the oscillations are represented by a pure standing wave (without a running component). It is worth noting that for the second harmonic of the resonator, the material density defect is defined by the following expression:

$$\rho \ = \ \rho_0 \ (1 \ + \ \varepsilon_2 \cdot cos2\varphi),$$

where ρ is the density of the material;

ρ_0 is the initial density;

ε is the relative defect size;

φ is the angle between the direction of vibration and one of the resonator's eigenaxes.

The value of the resonator frequency split is estimated by the formula:

$$\Delta\omega \ = \frac{8}{5} \varepsilon_2^2 \omega^2,$$

where $\Delta\omega$ is the natural frequency split;

ε is the relative defect size;

ω is the resonator frequency.

As we can see, the value of the frequency split is of the second order of magnitude with respect to the second harmonic of the defect. This means that the frequency splitting due to the first and third harmonics of the defect is also of the second order of magnitude. Therefore, when manufacturing the resonator, it is necessary to pay attention to the fourth harmonic of the defect, since this harmonic has a much stronger effect on the errors of the VARS than the others.

The frequency drift in the harmonic vibrations of a quartz gravity resonator (QGR) can be caused by an uneven distribution of damping sources in the resonator itself. Similar to the situation with the variation of the shell thickness, which leads to frequency splitting, which was discussed earlier, it is the fourth harmonic of the distribution of damping sources along the circumferential coordinate that creates a certain effect. However, an uneven distribution of damping sources can cause inhibition of resonator oscillations in the direction where these sources are located, which in turn can lead to a decrease in the Q-factor of the standing wave, especially in the areas where these sources are located.

The amplitudes of the damping components along the axes of the main damping sources (indicated in Fig. 2.3.2) decrease with time at certain rates. After complete attenuation of the components with a smaller damping time constant, a standing wave is established along the axis with the smallest damping time constant.

Fig. 2.3.2 shows a graph of depending on the wave angle θ, the frequency drift of the standing wave can have a sinusoidal shape, where the peak value is proportional to the difference in the damping time constants $\tau 1$ and $\tau 2$.

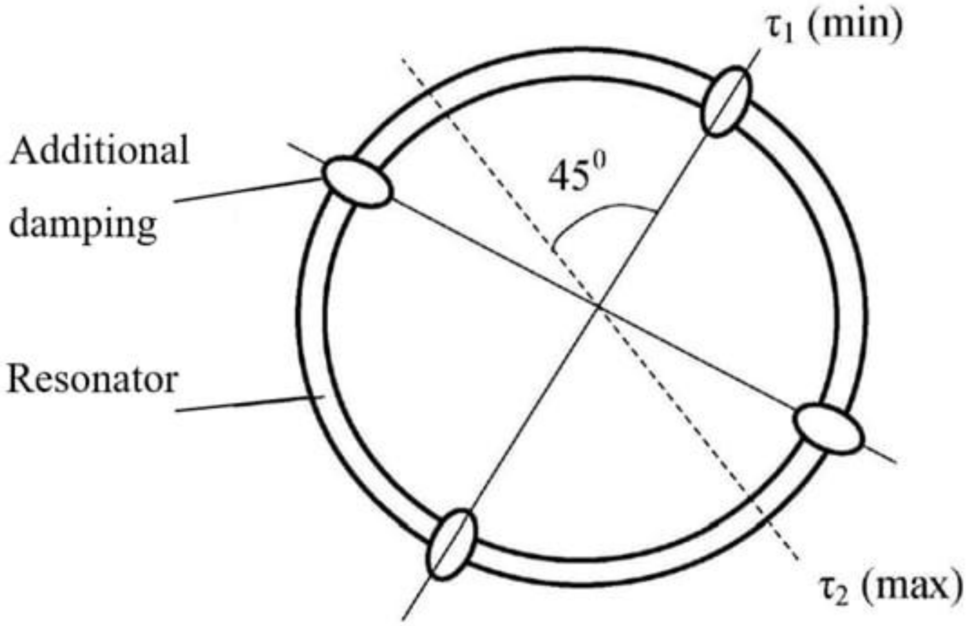

Fig. 2.3.2. Location of the damping axes

The sinusoidal curve's amplitude (Fig. 2.3.3), represented by its peak value, is inversely proportional to the difference in time constants:

$$\Delta\left(\frac{1}{\tau}\right) = \frac{1}{\tau_1} - \frac{1}{\tau_2} \approx \frac{\Delta Q}{Q}\frac{1}{\tau},$$

where τ_1 and τ_2 denote the minimum and maximum time constants of the resonator, respectively.

These time constants are defined as the damping time for the oscillation amplitude to decrease by e≈2.7 times. ΔQ represents the mismatch in the Q-factor. This systematic shift is commonly referred to as case-oriented or angle-dependent drift.

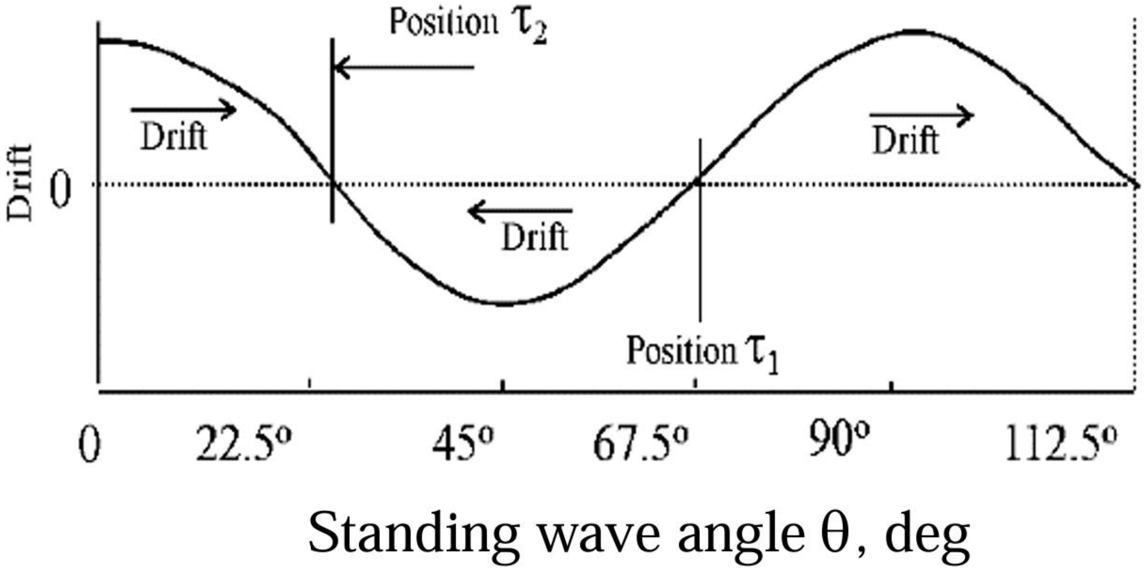

Fig. 2.3.3. The sinusoidal drift of the CGM, depending on the angle θ of the mine orientation relative to its body

Incidentally, manufacturing errors in MEMS devices lead to a stochastic variation in frequency splitting. Fig. 2.3.4 illustrates two-axis degenerate modes. The resonant frequency spans from 15,850 to 16,150 Hz, with a range of 300 Hz. Frequency splitting occurs within the range of 5 to 30 Hz, with an average value of 11.5 Hz [27].

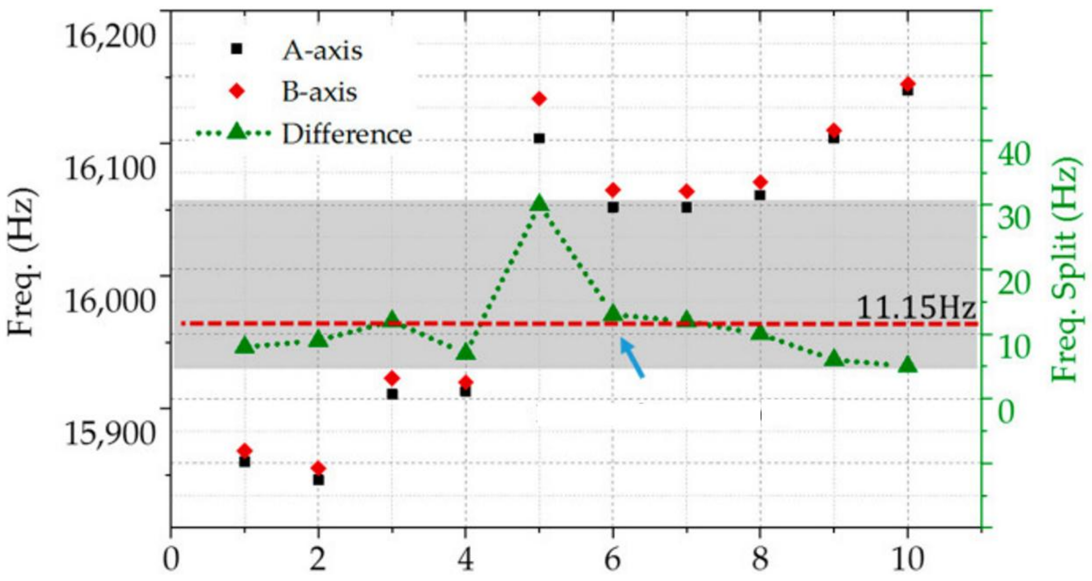

Fig. 2.3.4. The distribution of two-axis degenerate modes and frequency splits

2.4 Q-factor and frequency mismatches of rate-integrating gyroscopes

The Quality Factor (Q) stands out as one of the most crucial parameters for MEMS resonators, particularly in vibrating structures where precise monitoring of resonant frequency variation is imperative. A higher Q value signifies superior frequency resolution, underscoring the importance of Q factor measurement during testing, as it dictates the sensitivity of the micro-system.

In the design of resonant sensors, the readout circuit must strike a balance between low insertion loss and a high Q factor. Any output signal current resulting from coupling with the resonating sensor can dampen the mechanical resonance, highlighting the necessity for low energy dissipation.

Moreover, the measurement process itself can influence the Q factor of the gyroscope. The coupling of power from the resonator to generate a signal may lead to power dissipation. A high Q-factor indicates low energy dissipation, a critical parameter for assessing gyroscope performance. In multi-ring architectures, thermoelastic damping becomes significant for energy dissipation, particularly in high vacuum environments.

Gyroscopes can operate under mode match or mismatch conditions, affecting their dynamic performance and sensitivity stability across different operating temperatures. The varying slopes of resonant frequencies with ambient temperature can introduce frequency mismatch, impacting sensitivity stability.

Several techniques are available for measuring the Q-factor of MEMS resonators, including Transfer Function Measurement and Step Response Analysis. The latter method is typically more precise and suitable for tracking Q-factor changes.

Imperfections in manufacturing often lead to frequency and Q-factor variations among resonators, impacting their vibration modes. For instance, resonators may exhibit diverse resonant frequencies or Q-factors due to manufacturing irregularities [23].

MEMS resonators, despite their high accuracy and sensitivity, often face the problem of resonance frequency discrepancies. This can be the result of manufacturing imperfections or external factors. One important aspect of this problem is the mismatch of geometry, materials, or stresses in the resonator, which leads to variations in resonant frequencies.

These discrepancies can have a serious impact on the accuracy of sensors, signal filtering, and other aspects of their operation. For example, large input powers or signal amplitudes can create nonlinear effects and additional deviations in the frequency response of MEMS resonators.

The problem of frequency mismatch also arises from manufacturing variability, environmental influences, aging effects, and nonlinearities. Manufacturing processes can lead to variations in material dimensions and properties, as well as residual stresses that affect the resonant frequency. Environmental factors, such as temperature changes, humidity, pressure, and mechanical stress, can also change the frequency over time.

A variety of methods are used to address frequency mismatch. Design optimization plays a key role in fine-tuning the resonator geometry, material properties and structural characteristics to reduce frequency mismatch. Temperature compensation techniques, which use materials with known thermal properties or integrate temperature sensors for feedback, help to stabilize resonant frequencies under different conditions. Feedback control systems are also used to dynamically adjust operating parameters and ensure frequency stability. Advanced modelling techniques help to predict frequency fluctuations and optimize the design at the development stage. Rigorous testing and performance analysis during production also help to identify and reduce frequency variations.

In practical applications, frequency-matched MEMS resonators play a key role in stable oscillators, system synchronization and sensors. However, solving frequency mismatch problems requires a comprehensive approach, from design to implementation and calibration of MEMS-based systems [29].

2.5 Rate-integrating gyroscopes

The proposed Rate-Integrating Gyroscope (RIG) is designed based on the principle of frequency modulation (FM) gyroscope, where the eigenfrequency of each mode is modulated by the applied angular rate. This modulation serves as a fundamental aspect of integrating the gyroscope's output to determine the applied angle of rotation accurately.

Moreover, the RIG employs a resonator that is shared by both eigenmodes. This unique design allows for the simultaneous generation of two eigenmodes on the same resonator. This setup is crucial as it enables the RIG system to effectively cancel out the temperature-induced frequency changes. By doing so, the RIG can maintain high accuracy and stability even in varying temperature environments, making it suitable for precise angle measurement applications. The oscillation direction of the superposed linear motion, derived from the phase difference of the two eigenmodes, serves as the RIG's output signal, providing reliable angular rate information [23].

To create a block diagram (Fig. 2.5.1) of a frequency modulation (FM) velocity integration gyroscope, several key steps are required to ensure that the system components and their interconnections are fully represented.

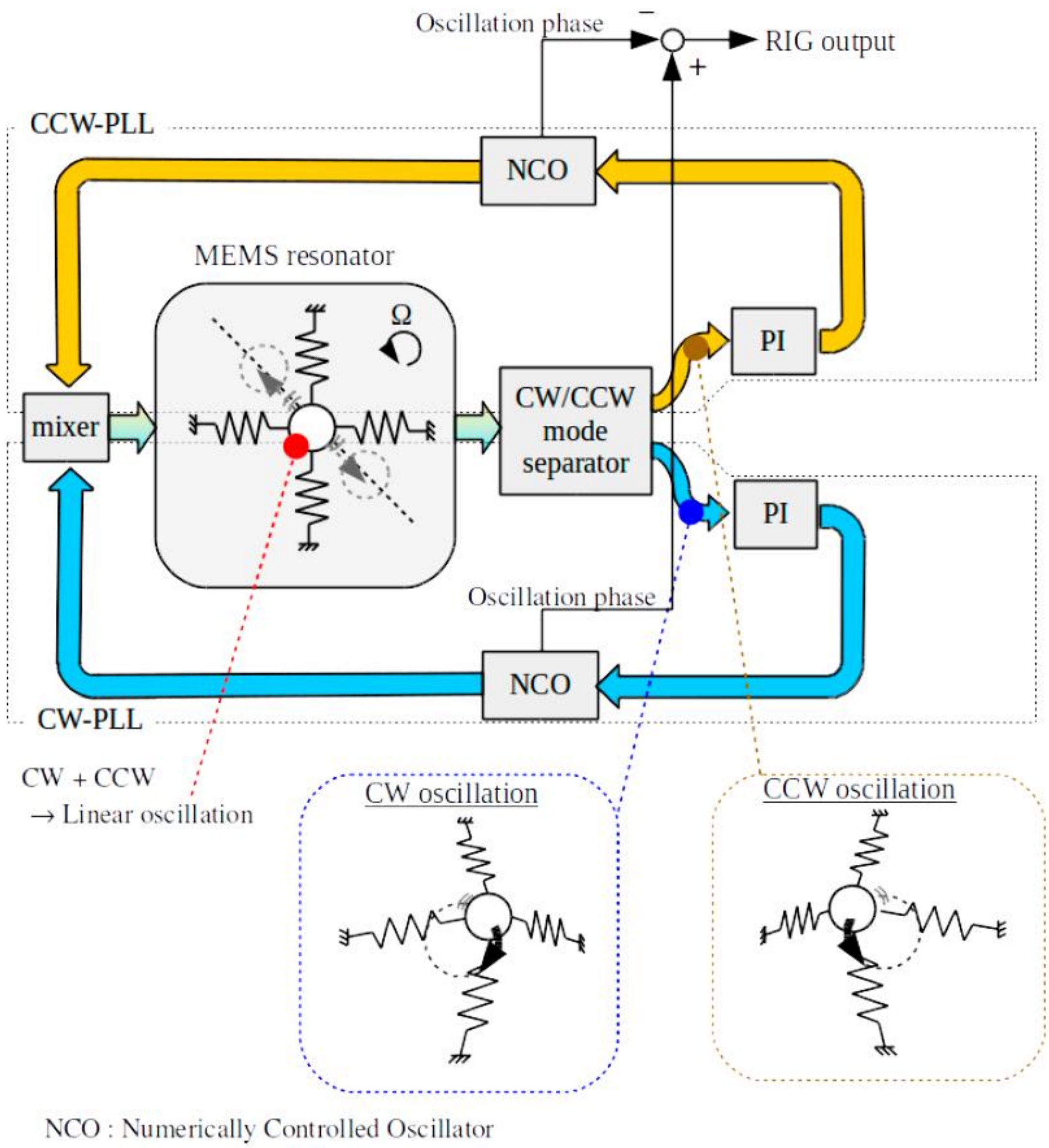

Fig. 2.5.1. Working principle of rate integrating gyroscope. Independently controlled CW and CCW mode oscillations are used to generate linear oscillation [4]. Mode coupling interferes CW and CCW modes, and thus generating measurement error

1.System analysis and requirements gathering: The requirements and specifications of the RIG system must be analyzed. This includes understanding the principles of FM gyroscope-based operation, identifying key components such as the common resonator and modulation circuits, and defining the desired output parameters.

2. Component identification: Based on the system analysis, the main components of the RIG system must be identified. This typically includes the resonator, modulation

circuits, signal processing unit, and any additional functions such as temperature compensation mechanisms or digital signal processing units.

3. Functional blocks and connections: Resonator block. Represents the common mode resonator and its operation in generating two eigenmodes simultaneously. Modulation circles block. Illustrates the modulation of natural frequencies based on an applied angular velocity. Signal Processing Block. Describes the processing of the modulated signal to obtain angular velocity information.

In example (Fig. 2.5.2) shows the rate-integrating gyroscope circuit, that use of an electromagnetic ring resonator (SGH-03, Silicon Sensing Systems Ltd.) as the main resonator, as well as a programmable field gate array (XC7A100T, Xilinx Inc., USA) together with analogue-to-digital and digital-to-analog converters as the controller [23].

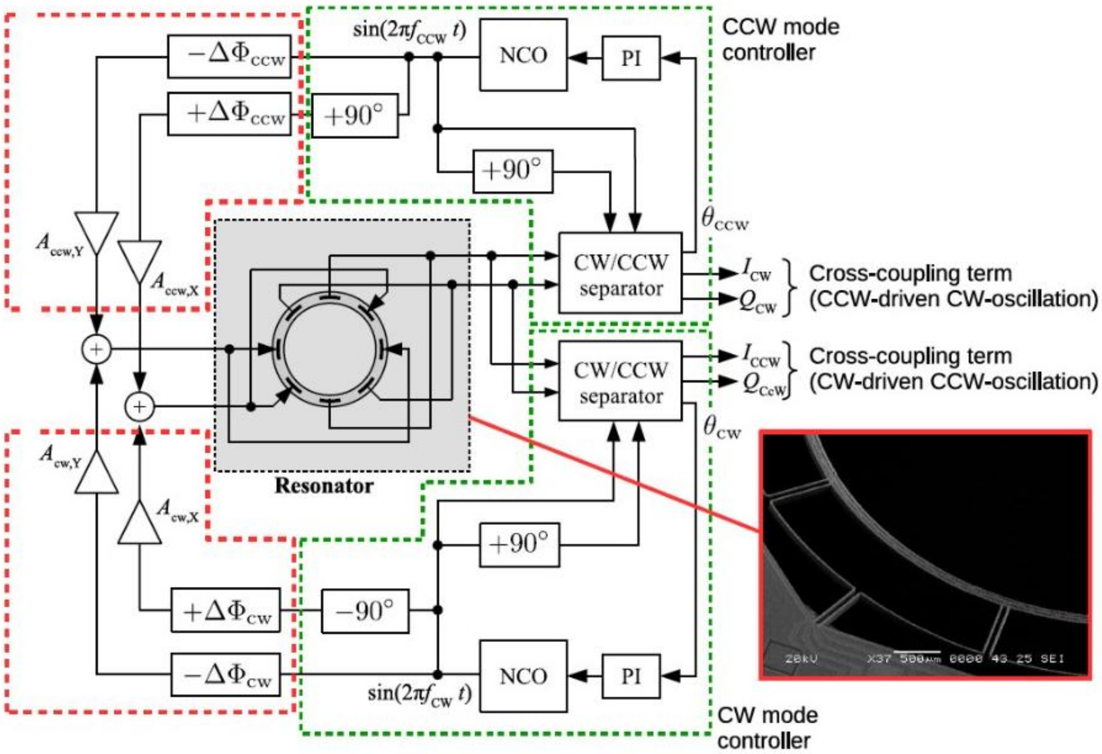

Fig. 2.5.2. System diagram of rate integrating gyroscope. Cross-coupling terms are detected by CW/CCW signal separators. Frequency and Q-factor mismatches are compensated by phases and amplitudes of driving signals

Periodic drift

Periodic drift is a systematic error that occurs periodically over time in the output signal of a gyroscope. In rate-integrated gyroscopes used to measure angular velocity or rotational velocity, periodic drift can affect their accuracy and reliability.

Periodic drift manifests itself as a cyclic change in the gyro output signal over time. Unlike random drift, which appears as a continuous and unpredictable change, periodic drift has a recognizable pattern or cycle.

Causes of periodic drift

Mechanical deformation. Changes in temperature or external influences, such as vibrations or shocks, can cause mechanical deformation in gyro components. For example, the expansion or contraction of materials due to temperature changes can alter their mechanical properties and lead to cyclic changes in the output signal.

Electrical conversions. The internal electrical components of the gyroscope, such as resistors, capacitors, or inductors, can be subject to cyclic changes due to temperature changes or electrical influences from external sources. This can lead to changes in the electrical characteristics of the gyroscope and periodic drift in the output signal.

Environmental influences. Electromagnetic fields, radiation, or other environmental factors can affect the operation of the electronic components of the gyroscope. For example, electromagnetic interference can cause intermittent changes in the output signal by interfering with the gyroscope's electronic circuits.

Impact on performance

Periodic drift introduces systematic errors in the gyro output signal, resulting in inaccurate measurements of angular velocity or rotational velocity. Long-term stability, which is important for applications such as navigation or stabilization systems, can be compromised by periodic drift. Periodic drift requires complex calibration procedures to reduce its effects, which increases system complexity and maintenance requirements.

Reduction strategies

Controlling the operating temperature of the gyro and its environment can reduce temperature-induced drift. Improved mechanical design, such as the use of high-quality materials and precision manufacturing techniques, can minimize drift associated with wear and tear. Shielding the gyro's electrical components from external electromagnetic interference can reduce electrically induced drift. Calibration algorithms, including periodic error correction procedures, can compensate for periodic drift during operation.

SECTION 3

RATE-INTEGRATING GYROSCOPE SIMULATION RESULTS

3.1. Two-dimensional pendulum model

To provide an adequate basis for the analysis of all CVG modes of operation, dynamic equations of oscillations should be generalized, including the components that determine the damping (Q-factor) and frequency (stiffness) mismatches and angular positions of their principal axes. Moreover, these equations should be convenient for engineering analysis and design of a control system for maintaining oscillations and measuring angle rate. Derivation of such generalized equations of the two-dimensional pendulum oscillations has been performed by D. Lynch for the mode n = 2. These equations, for the standing wave angle θ=0, are written as follows:

$$\ddot{x} - k\big(2\Omega\dot{y} + \dot{\Omega}y\big) + \frac{2}{\tau}\dot{x} + \Delta\left(\frac{1}{\tau}\right)(\dot{x}\cos 2\,\theta_\tau + \dot{y}\sin 2\,\theta_\tau) + (\omega^2 - k'\Omega^2)x - \omega\Delta\omega(x\cos 2\,\theta_\omega + y\sin 2\,\theta_\omega) = f_x;$$

$$\ddot{y} + k(2\Omega\dot{x} + \dot{\Omega}x) + \frac{2}{\tau}\dot{y} - \Delta\left(\frac{1}{\tau}\right)(-\dot{x}\sin 2\,\theta_\tau + \dot{y}\cos 2\,\theta_\tau) + (\omega^2 - k'\Omega^2)y + \omega\Delta\omega(-x\sin 2\,\theta_\omega + y\cos 2\,\theta_\omega) = f_y;$$

$$\omega^2 = \frac{\omega_1^2 + \omega_2^2}{2}; \frac{1}{\tau} = \frac{1}{2}\left(\frac{1}{\tau_1} + \frac{1}{\tau_2}\right); \omega\Delta\omega = \frac{\omega_1^2 - \omega_2^2}{2}; \Delta\left(\frac{1}{\tau}\right) = \frac{1}{\tau_1} - \frac{1}{\tau_2}; \#(3.1)$$

The parameters of equations (3.1) are shown in Fig. 3.1.1, where the scheme of a two-dimensional pendulum is presented. The mass m in Fig. 3.1.1 represents the elementary mass on the rim of the vibrating resonator; x and y are displacements along the X (primary) and the Y (secondary) resonator's axes; $\dot{\Omega}y$ and $\dot{\Omega}x$ are the angular acceleration; $k'\Omega^2$ is centripetal acceleration. There are also two axes with a minimum τ_1 and a maximum τ_2 damping time of free oscillations, which is equivalent to the minimum Q_1 and maximum Q_2 quality factor of the resonator, since $Q = \omega\tau/2$. These equations take into account that a resonator has two axes with a maximum ω_1 and a minimum ω_2 resonant frequencies. Moreover, the axis of the minimum resonant frequency has an angle θ_ω with the X direction of the primary oscillations, and the axis of the minimum quality factor is the angle θ_τ with the direction of the primary oscillations, as shown in Fig. 3.1.1. Forces f_x and f_y are a sum of control forces and forces arising due to the resonator's mass imbalance.

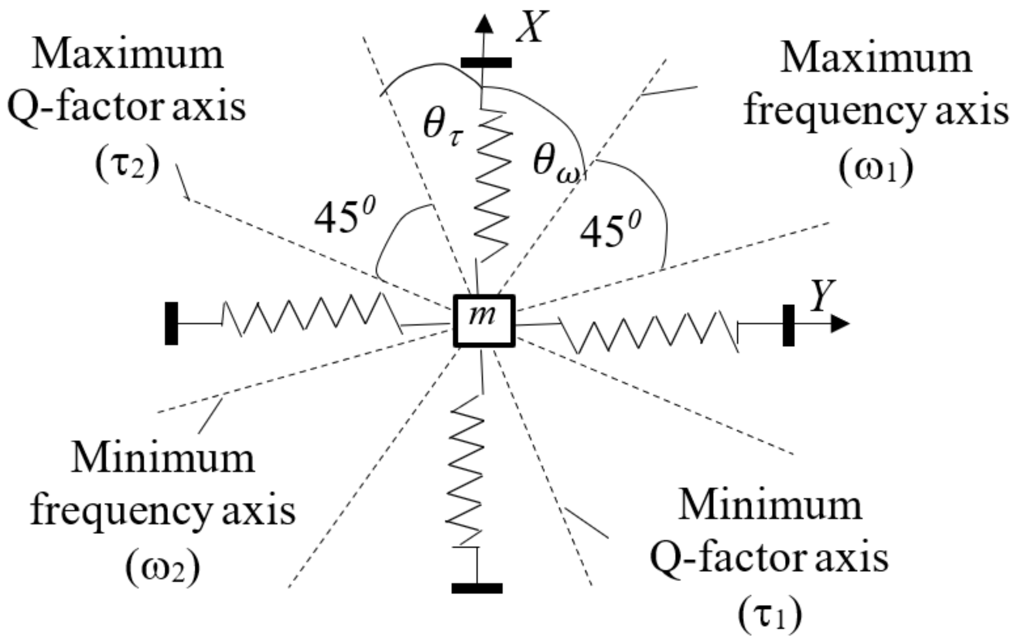

Fig. 3.1.1. Two-dimensional pendulum

Equations (3.1) are normalized on the vibrating mass, so the right and left parts of the equations have the dimension of linear acceleration, and the forces in the right parts are specific ones (normalized by mass).

These equations, which describe the oscillations of the primary mode along the *X*-axis and the secondary mode along the *Y*-axis, are called equations in fast variables, as deviations from the equilibrium position of the resonator elementary mass at both *X* and *Y* coordinates occur with a sufficiently high frequency close to resonant one.

The terms due to the presence of the angular acceleration $\dot{\Omega}$ and centripetal acceleration Ω^2 are also presented in these equations, which will not be taken into account in future considerations due to their negligible values in comparison to other terms. Indeed, $\dot{\Omega}x$ is less than $\Omega\dot{x}$ as many times as the resonant frequency is greater than the maximum frequency of change of the measured angle rate, i.e. up to 100 times. The maximum value of Ω^2 in most applications is also less than ω^2 approximately 100 times.

Since the *x* and *y* signals in equations (3.1) coming from the resonator are amplitude-modulated ones, with the carrier being the resonant frequency, and the angle rate the envelope, then to obtain information about the measured angle rate and to form control signals it is necessary to demodulate the signals of the *X* and *Y* sense electrodes. The demodulated signal components have a low frequency, so the equations for demodulated signals are called dynamic equations in "slow" variables. It is the behavior of the slow (i.e., demodulated) variables that simplifies error analysis.

To represent the dynamics of oscillations in slow variables, the transformations of fast variables *x*, *y* into the four slow variables C_x, S_x, C_y, S_y are being introduced by the following relations:

$$\begin{aligned} x(t) &= S_x cos\omega t + C_x sin\omega t; \\ y(t) &= S_y cos\omega t + C_y sin\omega t, \end{aligned} \#(3.2)$$

Substituting (3.2) in (3.1) and taking into account conditions for the existence of a standing wave in a resonator:

$$\begin{aligned} S_x cos\omega t + C_x sin\omega t &= 0; \\ S_y cos\omega t + C_y sin\omega t &= 0, \end{aligned} \#(3.3)$$

and after transformations and averaging over the period T=2π/ω of fast vibrations, taking into account the fact that during the period of fast vibrations the slow variables do not practically change, and the following relations are valid:

$$\frac{1}{T}\int_0^T sin\omega tdt = 0;\ \frac{1}{T}\int_0^T cos\omega tdt = 0;\ \frac{1}{T}\int_0^T sin^2\omega tdt = \frac{1}{2};$$
$$\frac{1}{T}\int_0^T cos^2\omega tdt = \frac{1}{2};\ \frac{1}{T}\int_0^T sin\omega t cos\omega tdt = 0\,. \#(3.4)$$

the four differential equations of the first order for slow variables can be obtained:

$$\dot{C}_x \approx -\frac{d_{xx}}{2}C_x + \frac{\omega_x^2 - \omega^2}{2\omega}S_x - \frac{d_{xy} - 2k\Omega}{2}C_y + \frac{k_{xy}}{2\omega}S_y - \frac{F_{xs}}{2\omega};$$
$$\dot{S}_x \approx -\frac{\omega_x^2 - \omega^2}{2\omega}C_x - \frac{d_{xx}}{2}S_x - \frac{k_{xy}}{2\omega}C_y - \frac{d_{xy} - 2k\Omega}{2}S_y + \frac{F_{xc}}{2\omega};$$
$$\dot{C}_y \approx -\ \frac{d_{xy} + 2k\Omega}{2}C_x + \ \frac{k_{xy}}{2\omega}S_x - \frac{d_{yy}}{2}C_y - \frac{\omega_y^2 - \omega^2}{2\omega}S_y - \frac{F_{ys}}{2\omega}; \#(3.5)$$
$$\dot{S}_y \approx -\frac{k_{xy}}{2\omega}\ C_x\ - \frac{d_{xy} + 2k\Omega}{2}S_x - \frac{\omega_y^2 - \omega^2}{2\omega}C_y - \frac{d_{yy}}{2}S_y + \frac{F_{yc}}{2\omega},$$

where

$$d_{xx} = \frac{2}{\tau} + hcos2(\theta - \theta_\tau);\ \ d_{yy} = \frac{2}{\tau} - hcos2(\theta - \theta_\tau);$$
$$d_{xy} = hsin2(\theta - \theta_\tau);) ;\ \ h = \frac{1}{\tau_1} - \frac{1}{\tau_2}; k_{xx} = \omega_1^2 - \omega\Delta\omega\ cos2(\theta - \theta_\omega); \#(3.6)$$
$$k_{yy} = \omega_1^2 + \omega\Delta\omega\ cos2(\theta - \theta_\omega);\ \ \ k_{xy} = -\omega\Delta\omega\ sin2(\theta - \theta_\omega).$$

Based on these designations, which have been written down for any arbitrary standing wave angle θ, the equations (3.1) can be rewritten in a more compact form:

$$\ddot{x} - 2k\Omega\dot{y} + d_{xx}\dot{x} + d_{xy}\dot{y} + k_{xx}x + k_{yy}y = f_x;$$
$$\ddot{y} + 2k\Omega\dot{x} + d_{yy}\dot{y} + d_{xy}\dot{x} + k_{yy}y + k_{xy}x = f_y. \#(3.7)$$

where d_{xx} is the X-axis damping coefficient;

d_{yy} is the Y-axis damping coefficient;

d_{xy} is a damping cross-coupling coefficient;

k_{xx} and k_{yy} are normalized by a mass resonator rigidity along the X and Y axes, respectively; k_{xy} are rigidity cross-coupling coefficient.

It is supposed that $d_{xy}=d_{yx}$ and $k_{xy}= k_{yx}$.

The demodulated slow variables C_x, S_x, C_y, S_y can be transformed into pendulum variables a, q, ϕ', and θ as follows:

$$a = \sqrt{\frac{1}{2}\left(E+\sqrt{E^2-Q^2}\right)};\, q = \sqrt{\frac{1}{2}\left(E-\sqrt{E^2-Q^2}\right)};$$

$$E = C_x^2+S_x^2+C_y^2+S_y^2;\ Q = 2(C_xS_y-C_yS_x); \qquad \#(3.8)$$

$$\theta = \frac{1}{2}arctan\frac{2\left(C_xC_y+S_xS_y\right)}{C_x^2+S_x^2-C_y^2-S_y^2};\phi' = \frac{1}{2}arctan\frac{2\left(C_xS_x+C_yS_y\right)}{C_x^2-S_x^2+C_y^2-S_y^2};$$

In the rate-integrating mode, a CVG's control system should provide to perform only three next equalities:

$$E = a^2 = const;\ \phi' = 0; q = 0. \#(3.9)$$

3.2. Rate-integrating control system block diagram

The Rate-integrating or whole angle mode principle of operation has been described in subsection 3.1, here the control system block diagram of this mode will be described in the case of ring electrode absence. Rate-integrating CVG errors will be discussed in more detail. Simulation and measurement results will be presented for low Q-factor and unbalanced by Q-factor mismatch resonator CVGs.

The block diagram of the standing wave control system in the rate-integrating (whole angle) mode without the use of a ring electrode is presented in Fig. 3.2.1.

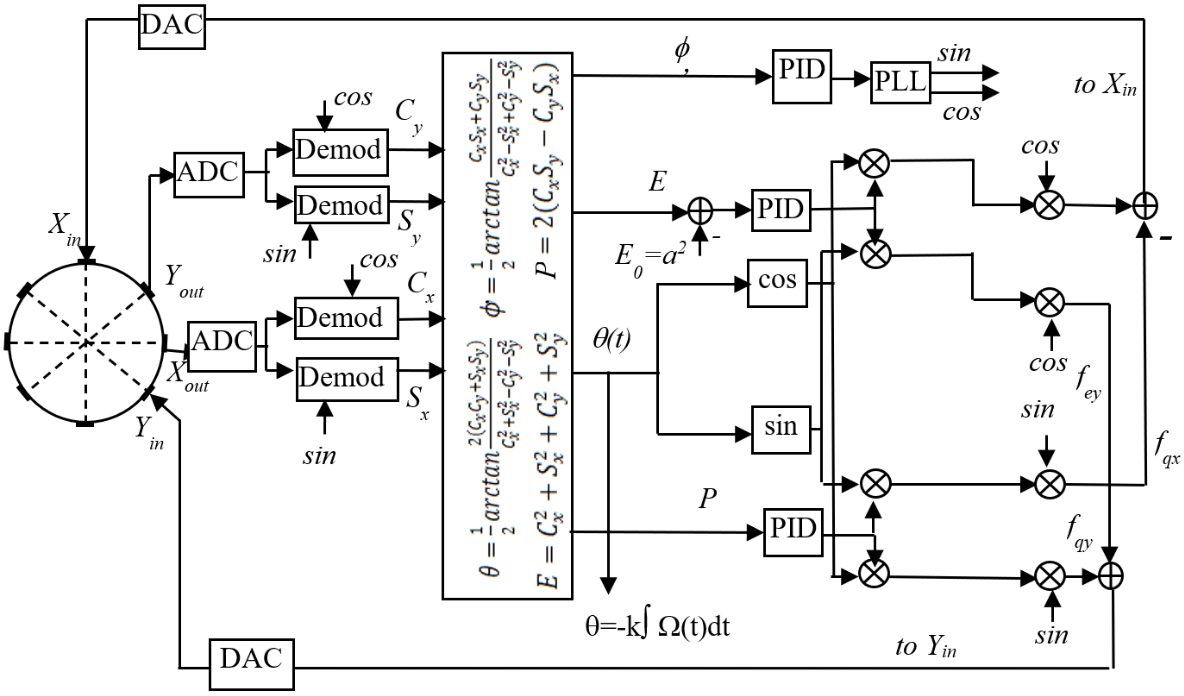

Fig. 3.2.1. Rate-Integrating CVG control system block diagram

Based on this block diagram was built a Simulink model that, in the form of the blocks, is shown in Fig. 3.2.2.

Fig. 3.2.3 shows the results of measuring a rotation angle by the model presented in Fig. 3.3, operating in rate-integrating mode under the constant actual angle rate of 813.57 deg/s.

Fig. 3.2.3 shows a straight line 1 that represents the true angle of rotation, and curve 2 is the output signal of the rate-integrating CVG with a measurement error that depends on the standing wave angle θ.

As can be seen from Fig. 3.2.3 *b*, maximum value of periodic angle drift is about 6 deg. This periodic drift can be corrected.

Fig. 3.2.4 shows the residual error after correction by wave angle θ. An expression for error correction is presented to be:

$$C(\theta) = 0.1063\sin(2\theta - 0.1947) + 0.006\sin(4\theta - 0.7848) - 0.0052\sin(0.2222\theta + 1.2372) - 0.0052\ \text{rad.} \quad (3.10)$$

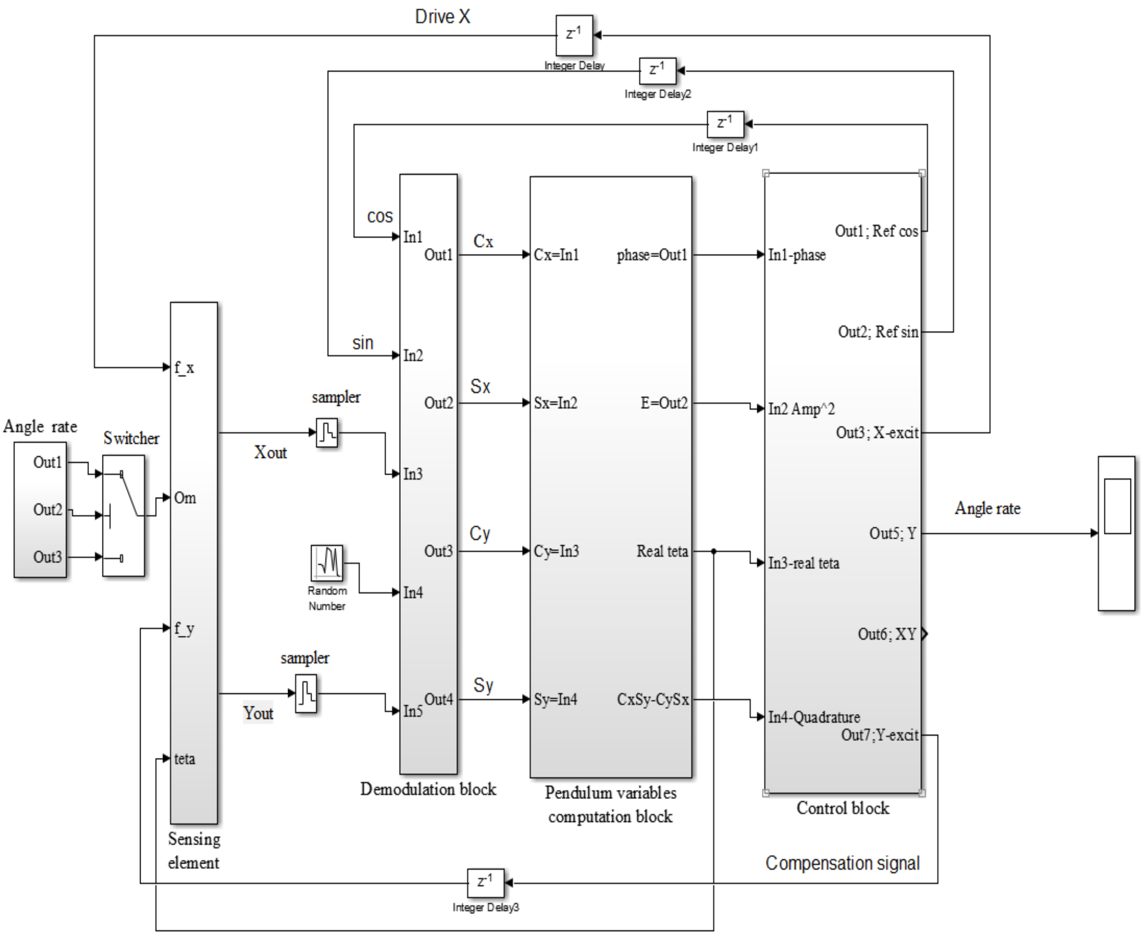

Fig. 3.2.2. CVG model in designations of Simulink blocks

An RMS correction error is equal to $\delta\alpha$=0.068 deg. when measuring an angle of about 250 deg.

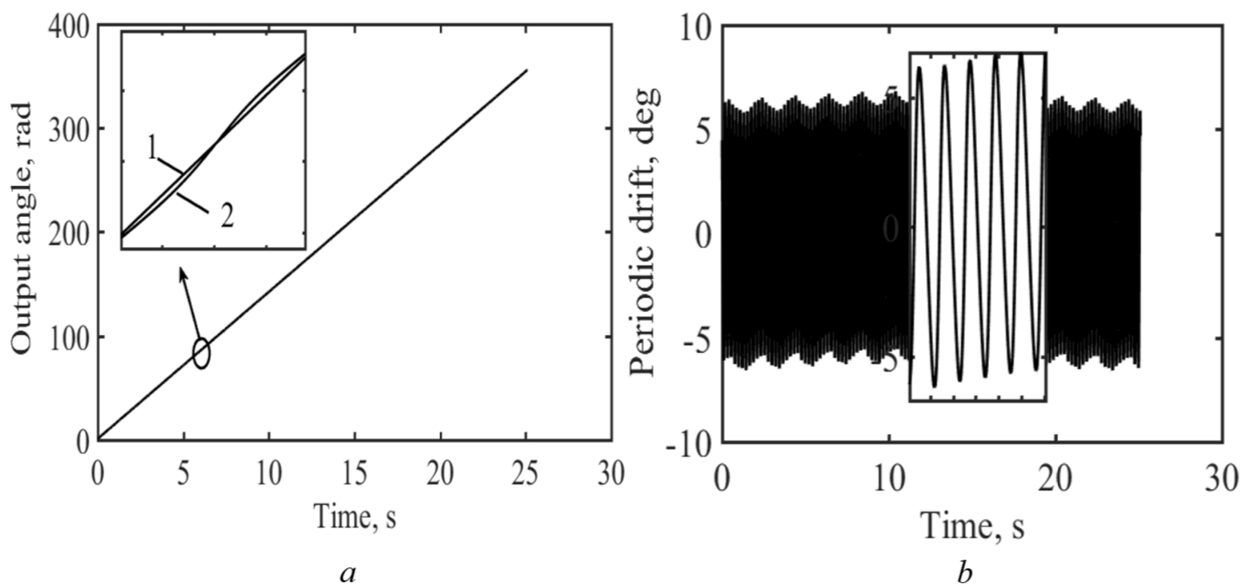

Fig. 3.2.3. Rate-integrating CVG with virtual rotation (*a*) and its periodic drift (*b*)

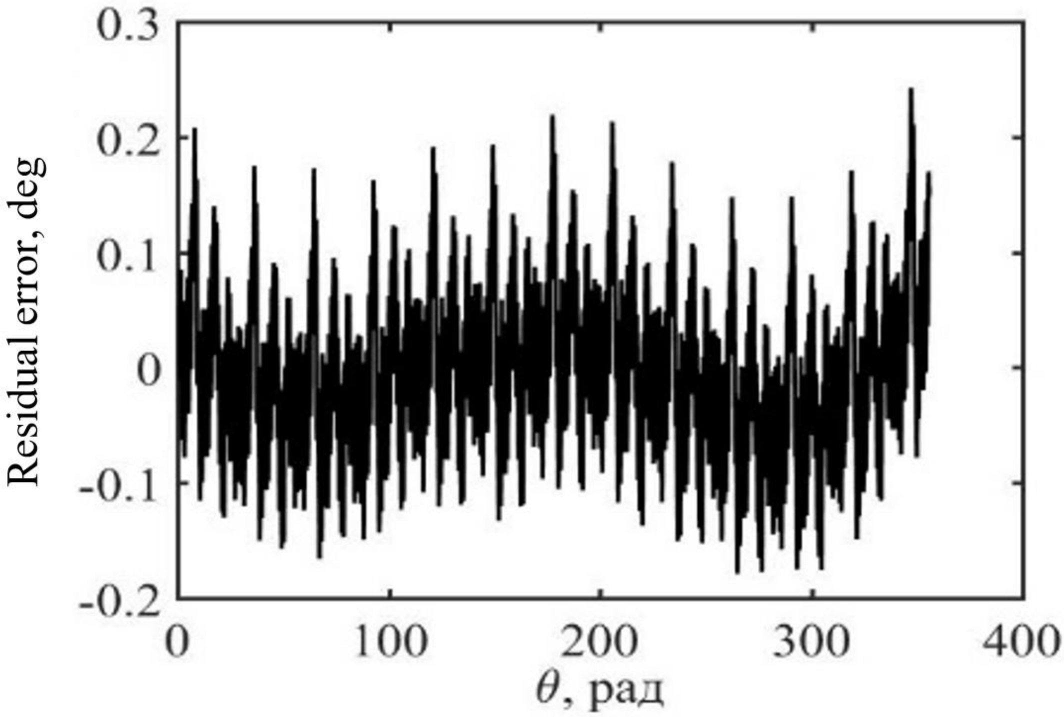

Fig. 3.2.4. The residual periodic drift after correction

A rate-integrating CVG has advantages over the other modes of its operation when measuring large and ultra-large angle rates and angles of rotation. It also has higher bandwidth and stable scale factor.

3.3. Conclusion

Coriolis vibratory gyroscope (CVG) is one of the chronologically latest gyroscopic technologies that appeared on the world market in the 90s of the last centuries. This technology has spread throughout the world for a relatively short time, mainly due to its microminiature version based on the micro-electro-mechanical system (MEMS), the so-called MEMS gyroscopes.

There are three modes of CVG operation: fist mode is a force-rebalance mode or rate mode, when the gyroscope measures angle rate relative to the inertial space. The second mode is rate-integrating mode or whole angle mode, where gyroscope measures angle of rotation relative to the inertial space. The third mode is a differential mode, where gyroscope has two measurement channels, which measure plus and minus angle rate ($\pm\Omega$), simultaneously, and difference of the two channels measurements increases useful signal.

The rate-integrating mode of operation has some advantages over others under measuring the angle of rotation at high angle rate, because it has stable scale factor and high bandwidth. Therefore, it will have low dynamic error.

The periodic error inherent to the rate-integrating mode of operation can be effectively corrected by the standing wave angular position relative to the drive electrode.

CONCLUSION

Coriolis vibratory gyroscope (CVG) is one of the chronologically latest gyroscopic technologies that appeared on the world market in the 90s of the last centuries. This technology has spread throughout the world for a relatively short time, mainly due to its micro-miniature version based on the micro-electro-mechanical system (MEMS), the so-called MEMS gyroscopes.

Significant prospects for the development of high-precision vibratory gyroscopy in the world are expected due to the transition to axisymmetric MEMS resonators, which are shells of bodies of rotation. Advanced gyroscopic countries of the world are currently actively working in this direction.

MEMS gyros can also operate in three modes of operation – in the rate mode, in the whole-angle mode or rate-integrating mode, and in differential mode. Each mode of operation has advantages and disadvantages. The rate-integrating mode of operation has advantages over other modes by scale factor stability, wide bandwidth and high dynamic range.

All three modes of operation can be realized for low-cost MEMS gyroscopes, with automatic switching from one mode to another, providing versatility in measuring angle rates and rotation angles under changing conditions of motion and environment.

REFERENCES

1. MEMS (Micro Electro Mechanical System) [Electronic resource]. URL: https://engineeringproductdesign.com/mems-micro-electro-mechanical-system/
2. What is MEMS? [Electronic resource]. URL: https://www.mems-exchange.org/MEMS/what-is.html
3. Micro-electromechanical systems (MEMS) [Electronic resource]. URL: https://www.techtarget.com/iotagenda/definition/micro-electromechanical-systems-MEMS
4. MEMS (Micro Electro Mechanical System) [Electronic resource]. URL: https://engineeringproductdesign.com/mems-micro-electro-mechanical-system/
5. MEMS Accelerometers [Electronic resource]. URL: https://www.siliconsensing.com/technology/mems-accelerometers/#:~=MEMS%20accelerometers%20are%20used%20wherever,whatever%20they%20are%20attached%20to
6. Guide to Microphones in Product Design [Electronic resource]. URL: https://engineeringproductdesign.com/knowledge-base/guide-to-microphones-in-product-design/
7. Gyroscope [Electronic resource]. URL: https://byjus.com/physics/gyroscope/
8. Gyroscope [Electronic resource]. URL: https://testbook.com/physics/gyroscope
9. What is MEMS Gyroscope [Electronic resource]. URL: https://www.linkedin.com/pulse/what-mems-gyroscope-kelly-yu-tflfc/
10. MEMS Gyroscope [Electronic resource]. URL: https://www.ericcointernational.com/info/mems-gyroscope.html
11. How is MEMS Different from Mechanical Gyroscope [Electronic resource]. URL: https://medium.com/@ericcointernational001/how-is-mems-different-from-mechanical-gyroscope-ea95ad6435f4 Excitation. Microsystem Technologies. DOI: 10.1007/s00542-022-05391-9

12. Wang, W., Zhang, Y., Chen, Z., & Ren, H. (2022). Study of Piezoelectric MEMS Energy Harvester with Parametric Excitation. Microsystem Technologies. DOI: 10.1007/s00542-022-05391-9
13. Damodaran, V., Ranji, A.R., Li, K., Chen, Z., Alirezaee, S., & Ahamed, M.J. (2022). MEMS-Based Inertial Sensors for Navigation Applications: A Review. Micromachines, 13, 2195. DOI: 10.3390/mi13122195
14. Resonators. SiTime. [Electronic resource]. URL: https://www.sitime.com/products/resonators
15. Inertial Navigation System. Wikipedia. [Electronic resource]. URL: https://en.wikipedia.org/wiki/Inertial_navigation_system
16. Zhang, L., Zhao, Y., & Li, X. (2015). MEMS-Based Capacitive Pressure Sensors with Different Sensing Capacitor Configurations. Micromachines, 6(2), 175. DOI: 10.3390/mi6020175
17. Sun, H., Zhou, T., & Zhao, J. (2022). Recent Advances in MEMS-Based Microfluidic Devices for Biomedical Applications. Micromachines, 15(2), 175. DOI: 10.3390/mi15020175
18. Ranji, A.R., Damodaran, V., Li, K., Chen, Z., Alirezaee, S., & Ahamed, M.J. (2022). Recent Advances in MEMS-Based 3D Hemispherical Resonator Gyroscope (HRG)—A Sensor of Choice. Micromachines, 13, 1676.
19. A 3D Biased Resonator: Stationary Eigenfrequency Frequency Domain and Pull-in Analysis [Електронний ресурс].
20. Casset, F., et al. (2009). 3D Multi-Frequency MEMS Electromechanical Resonator Design. In EuroSimE 2009 - 10th International Conference on Thermal, Mechanical and Multi-Physics Simulation and Experiments in Microelectronics and Microsystems, Delft, Netherlands, pp. 1-5.
21. Feng, T., Yuan, Q., Yu, D., Wu, B., & Wang, H. (2022). Concepts and Key Technologies of Microelectromechanical Systems Resonators. Micromachines, 13(12), 2195.
22. Morris, A. S., & Langari, R. (2021). Rotational Motion Transducers. In Measurement and Instrumentation (Third Edition).

23. Tsukamoto, T., & Tanaka, S. (2019). Automated Frequency and Quality Factor Mismatch Compensation Method for MEMS Rate Integrating Gyroscope. In Proceedings of the 20th International Conference on Solid-State Sensors, Actuators and Microsystems and Eurosensors XXXIII, TRANSDUCERS 2019 and EUROSENSORS XXXIII (pp. 1831-1834). Institute of Electrical and Electronics Engineers Inc.
24. Gregory, J. A., Cho, J., & Najafi, K. (2011). MEMS Rate and Rate-Integrating Gyroscope Control with Commercial Software Defined Radio Hardware. In Proceedings of the 16th International Solid-State Sensors, Actuators and Microsystems Conference, Beijing, China (pp. 2394-2397).
25. Chikovani, V. V., Sushchenko, O. A., Azarskov, V. M., Bezkorovainyi, Y. M., Korolov, V. M., & Korolova, O. V. (2020). Errors Compensation of Ring-Type MEMS Gyroscopes Operating in Differential Mode. In Proceedings of the 2020 IEEE XVIth International Conference on the Perspective Technologies and Methods in MEMS Design (MEMSTECH), Lviv, Ukraine (pp. 68-71).
26. Chikovani, V., Tsiruk, H., & Korolova, O. (2018). Triple-Mode Vibratory Gyroscope. Military Technical Collection, Hetman Petro Sahaidachnyi National Army Academy, Lviv, Ukraine, No. 18, pp. 18–24.
27. Jiang, B., Su, Y., Liu, G., Zhang, L., & Liu, F. (2020). A High Q-Factor Outer-Frame-Anchor Gyroscope Operating at First Resonant Mode. Micromachines, 11, 1071.
28. Mathias, H., Parrain, F., Gilles, J.-P., Megherbi, S., Zhang, M., Coste, P., & Dupret, A. (2007). Architecture for Integrated MEMS Resonators Quality Factor Measurement. In Proceedings of DTIP, pp. 25–27.
29. Tsukamoto, T., & Tanaka, S. (2021). Theoretical Consideration of Mismatch Compensation for MEMS Resonator Having Unaligned Principle Axes. In Proceedings of the 2021 IEEE International Symposium on Inertial Sensors and Systems (INERTIAL), Kailua-Kona, HI, USA (pp. 1-4).